Dynamics of black holes in dense stellar systems

Sambaran Banerjee
Helmholtz-Instituts für Strahlen- und Kernphysik (HISKP) and
Argelander-Institut für Astronomie (AlfA), University of Bonn

@ The Astronomical Institute
Charles University of Prague

Lecture 1

UNIVERSITÄT BONN

DFG Deutsche Forschungsgemeinschaft

Contents

- Introduction: gravitational waves, detectors, basics of stellar dynamics - mass segregation, energy equipartition, core collapse

- Dynamics of stellar mass black holes in clusters: dynamical mechanisms of general-relativistic in-spirals and their observational signatures.

- Effect of black holes on cluster evolution and dynamics, N-body codes, stellar evolution and remnant formation in N-body codes (the BSE framework)

What is a black hole?

- Relativist's definition: a surface where a photon "continues to stay" and a massive particle can only travel inwards.

- Called a "null hypersuface" or event horizon.

- Necessarily spherically symmetric or axisymmetric in a static spacetime --- 'no-hair theorem'.

- Mathematically well-studied.

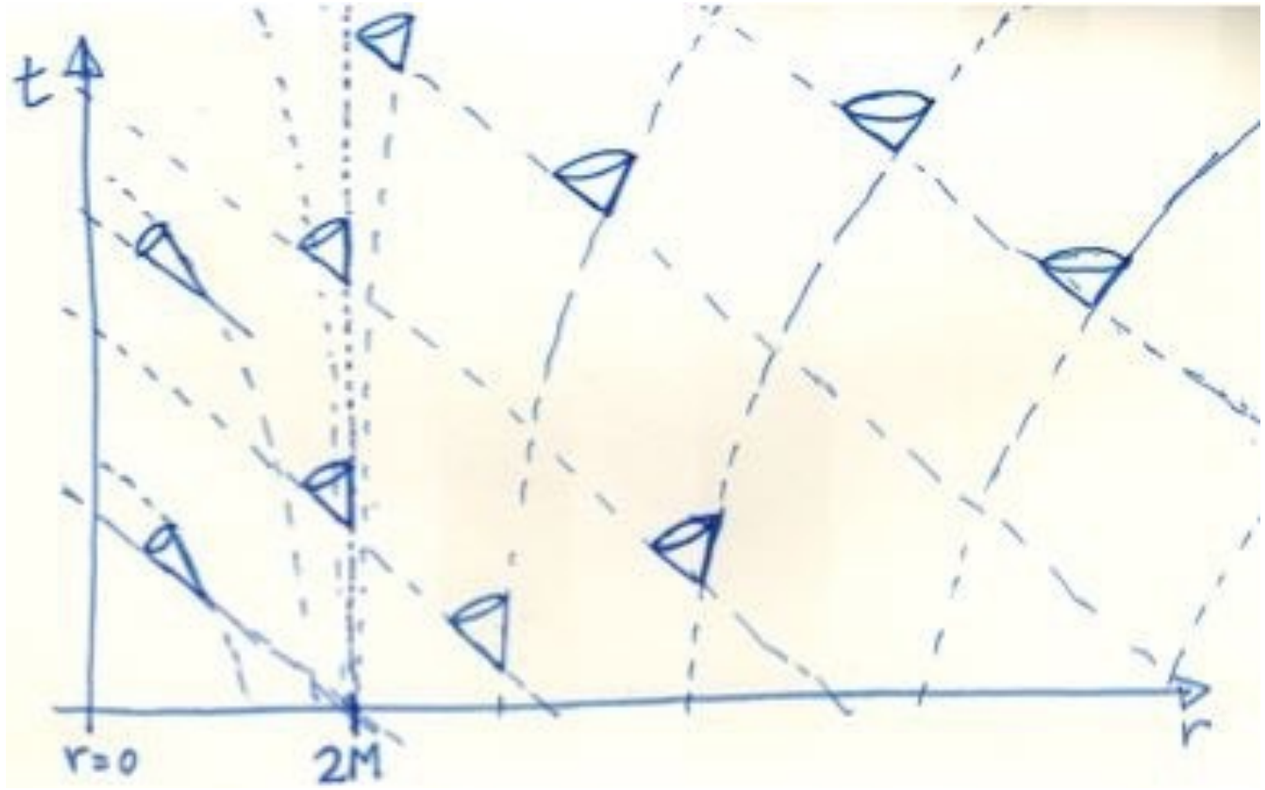

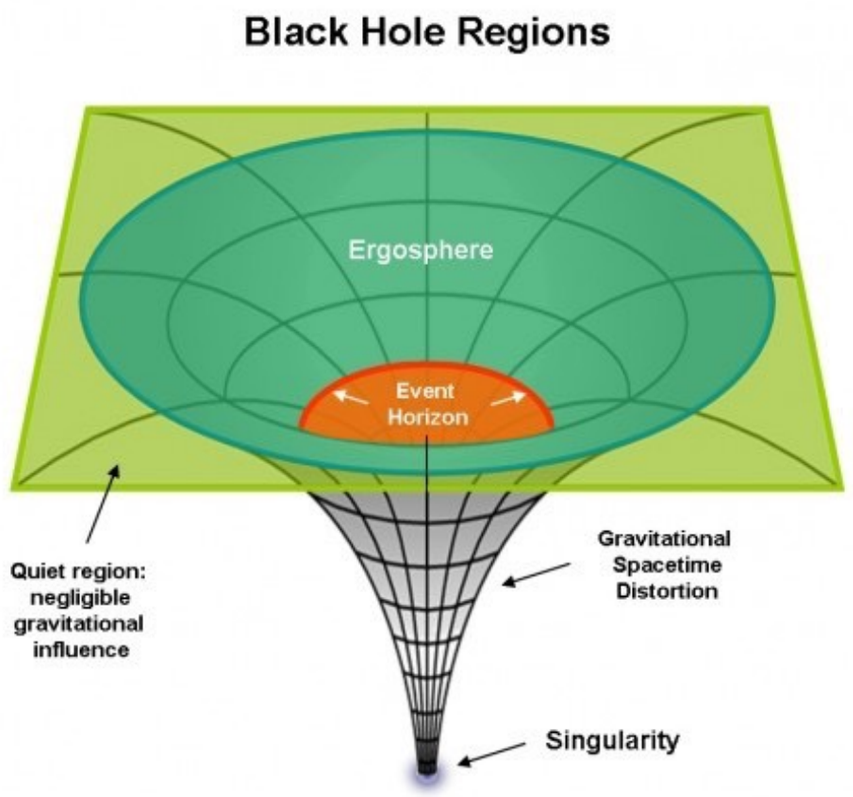

What is a real (astrophysical) black hole?

Any self-gravitating object that is more massive than $\gtrsim 3M_\odot$ and is "compact".

Compact => supporting pressure is degeneracy pressure (e.g., white dwarf and neutron star)

Beyond $\approx 3M_\odot$ (the maximum mass of a Neutron Star) there is no known way to support against self-gravitational collapse (unless an energy source is available) - and endless collapse of matter towards a black hole is assumed.

What is a real (astrophysical) black hole?

Any s $3M_\odot$
and is

Comp re
(e.g., v

Beyon r)
there onal
collap dless
collap

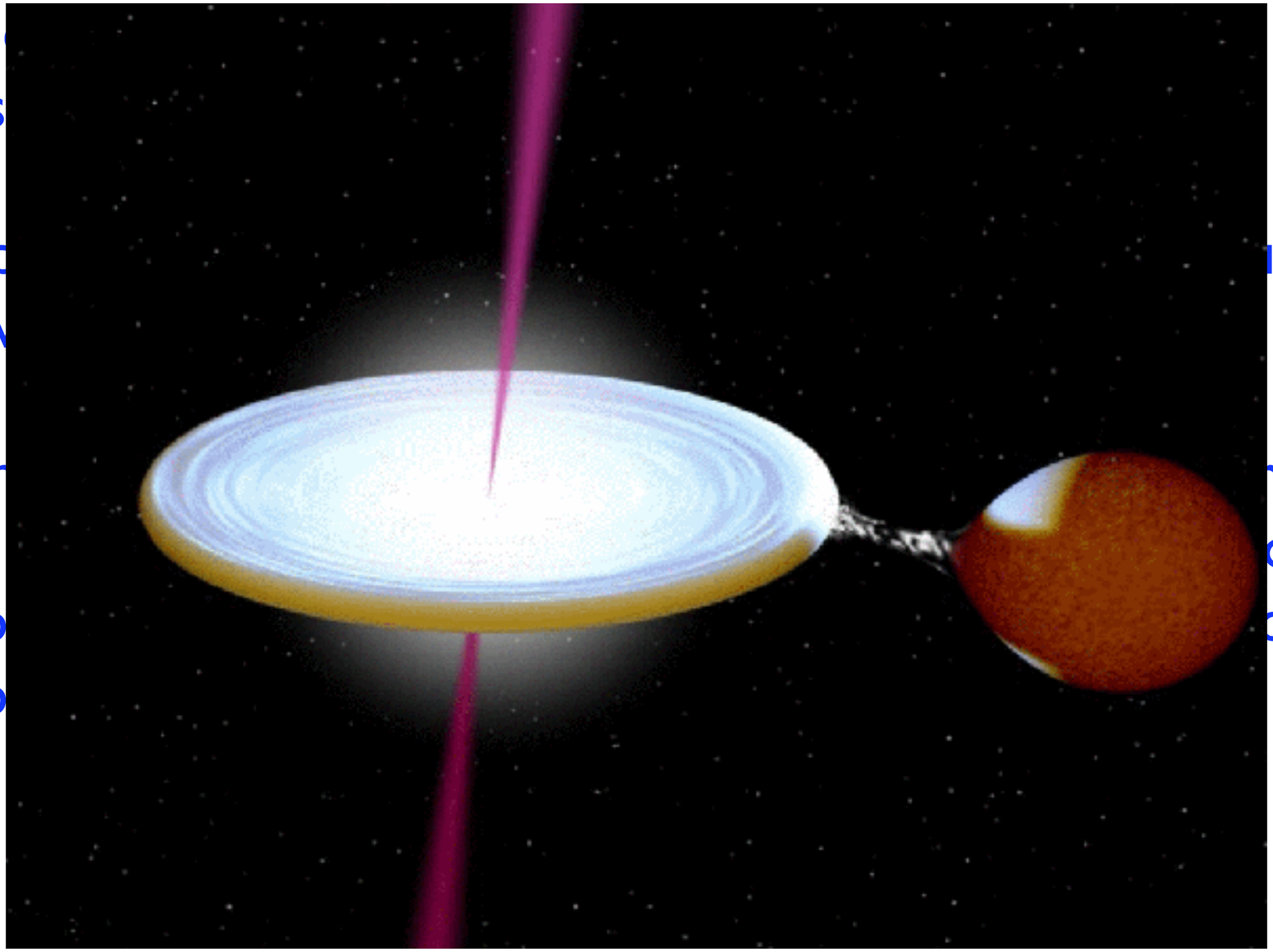

What is a real (astrophysical) black hole?

Any self-gravitating object that is more massive than $\gtrsim 3M_\odot$ and is "compact".

Compact => supporting pressure is degeneracy pressure (e.g., white dwarf and neutron star)

Beyond $\approx 3M_\odot$ (the maximum mass of a Neutron Star) there is no known way to support against self-gravitational collapse (unless an energy source is available) - and endless collapse of matter towards a black hole is assumed.

Celestial black holes: wide (inferred) mass-range

- Stellar mass black holes (BH) $M_{BH} < 100 M_\odot$
  --- end products of massive stars.

- Intermediate mass black holes (IMBH) (?)
  $\sim 10^2 M_\odot - \sim 10^4 M_\odot$ *--- existence still unclear!*
  formed via runaway merger of stars in clusters, gas accretion by seed stellar BHs, direct collapse of massive 'first stars'.

- Supermassive black holes (SMBH) $M_{BH} > 10^5 M_\odot$
  galaxies' central engines, e.g., active galactic nuclei, radio galaxies: possible formation by matter infall at galaxy center, galaxy-galaxy mergers

First *direct* detection of gravitational waves GW150914

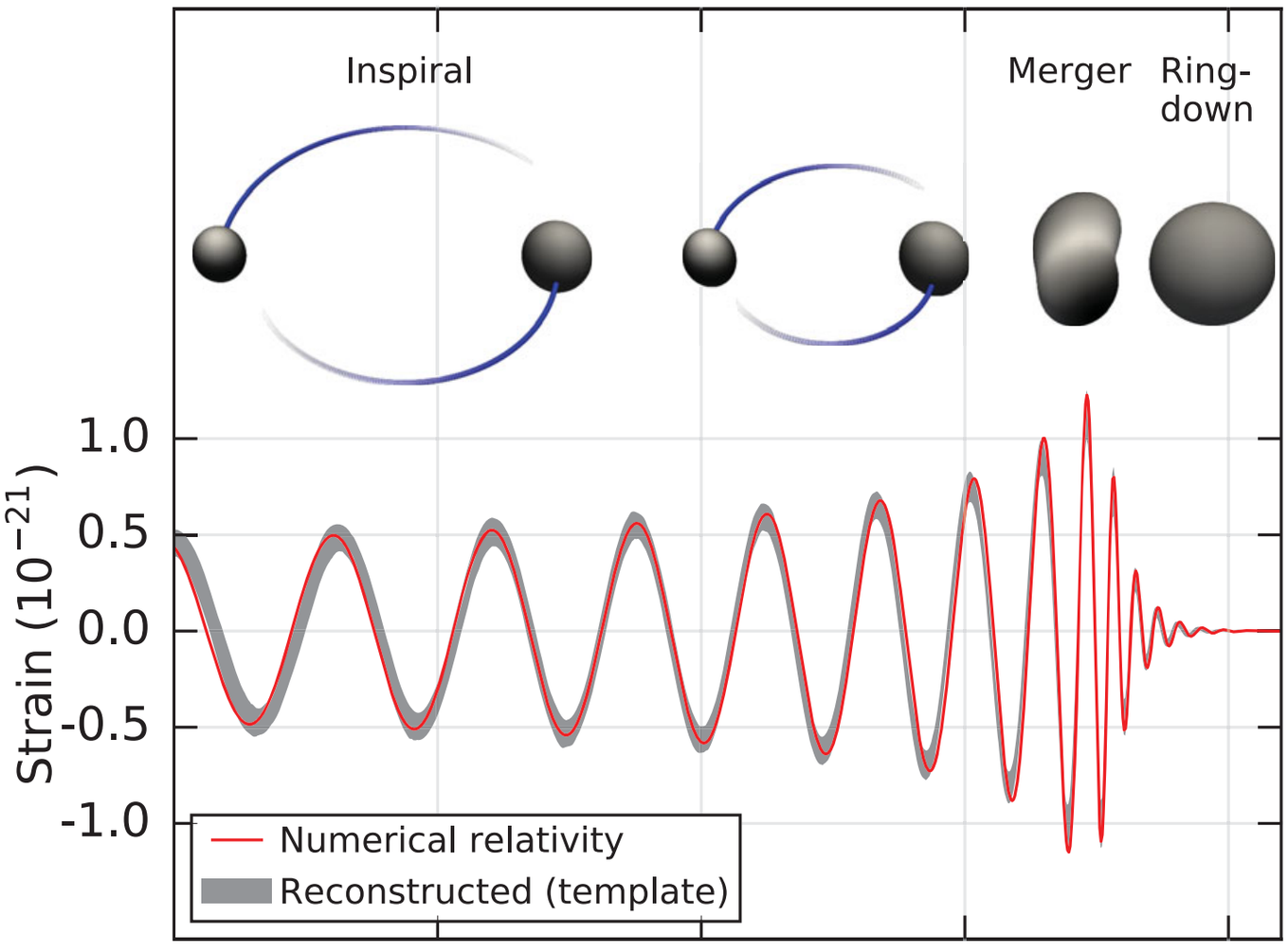

[From LIGO Scientific Collaboration PRL 116, 061102 (2016)]

Direct detection of gravitational-waves (GW) from merging binary black holes is the most unambiguous detection of black holes and its parameters (mass, spin) and, of course, the best proof of Einstein's general relativity.

The best and the strongest proof of Einstein's general theory of relativity, to date.

A very strong if not the best evidence so far of the existence of black holes.

Paves the most unambiguous way to weigh black holes and measure their spins through the same measurement.

The 2017 Nobel Prize in Physics (to Rainer Weiss, Barry Barish, and Kip Thorne of the LIGO-VIRGO Collaboration)

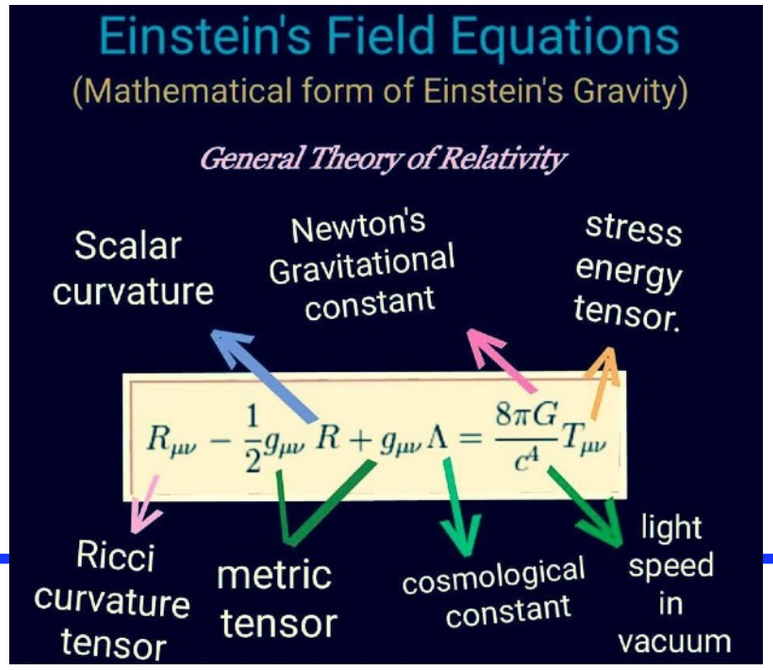

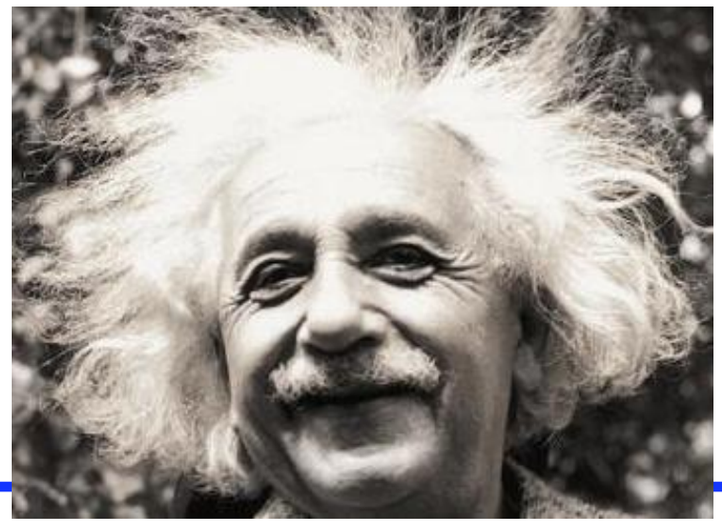

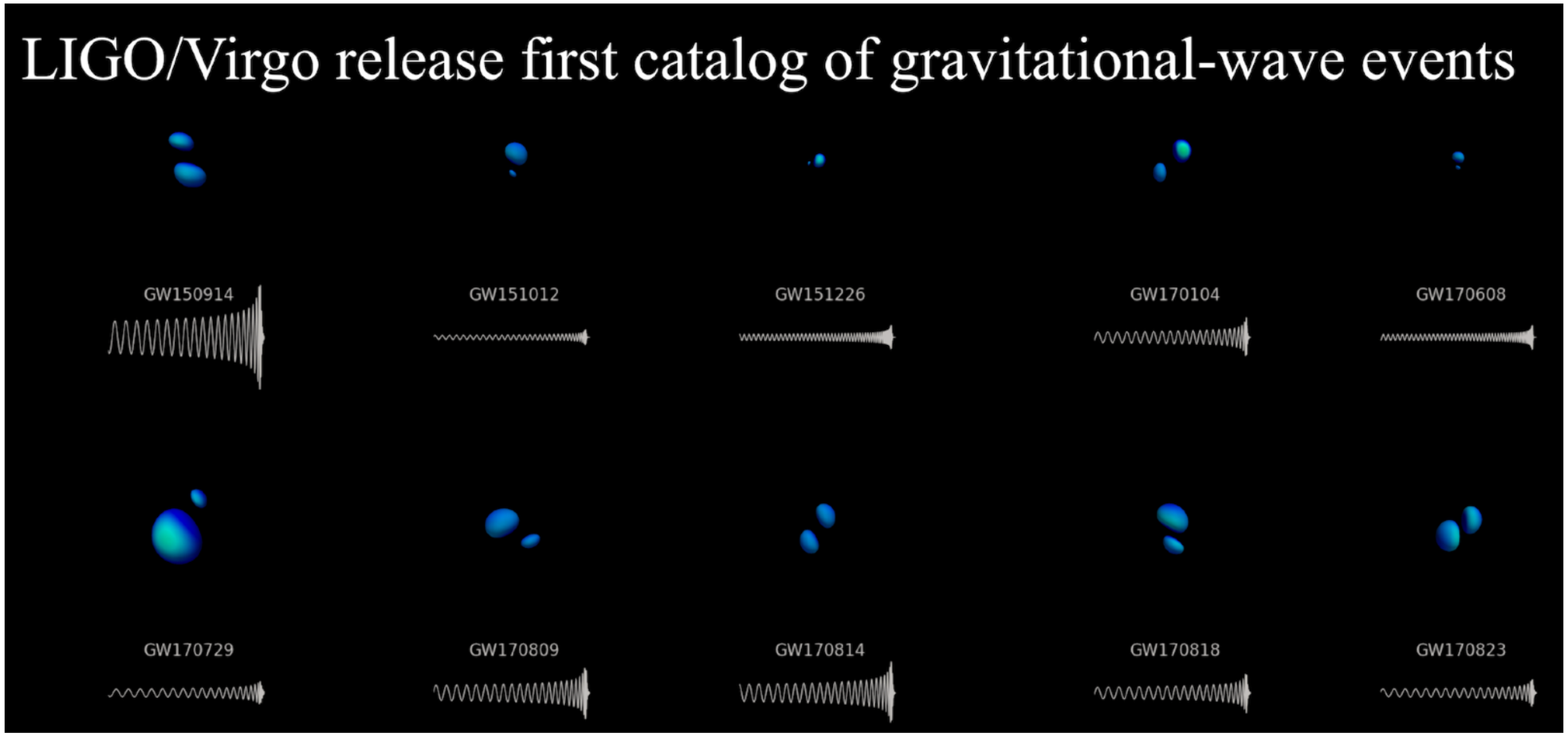

LVC until second observing run (O2): Phys. Rev. X 9, 031040 (2019)

Event	$m_1/M_\odot$	$m_2/M_\odot$	$\mathcal{M}/M_\odot$	$\chi_{\rm eff}$	$M_f/M_\odot$	a_f	$E_{\rm rad}/(M_\odot c^2)$	$\ell_{\rm peak}/({\rm erg\,s^{-1}})$	$d_L/{\rm Mpc}$	z	$\Delta\Omega/{\rm deg}^2$
GW150914	$35.6^{+4.7}_{-3.1}$	$30.6^{+3.0}_{-4.4}$	$28.6^{+1.7}_{-1.5}$	$-0.01^{+0.12}_{-0.13}$	$63.1^{+3.4}_{-3.0}$	$0.69^{+0.05}_{-0.04}$	$3.1^{+0.4}_{-0.4}$	$3.6^{+0.4}_{-0.4}\times10^{56}$	440^{+150}_{-170}	$0.09^{+0.03}_{-0.03}$	182
GW151012	$23.2^{+14.9}_{-5.5}$	$13.6^{+4.1}_{-4.8}$	$15.2^{+2.1}_{-1.2}$	$0.05^{+0.31}_{-0.20}$	$35.6^{+10.8}_{-3.8}$	$0.67^{+0.13}_{-0.11}$	$1.6^{+0.6}_{-0.5}$	$3.2^{+0.8}_{-1.7}\times10^{56}$	1080^{+550}_{-490}	$0.21^{+0.09}_{-0.09}$	1523
GW151226	$13.7^{+8.8}_{-3.2}$	$7.7^{+2.2}_{-2.5}$	$8.9^{+0.3}_{-0.3}$	$0.18^{+0.20}_{-0.12}$	$20.5^{+6.4}_{-1.5}$	$0.74^{+0.07}_{-0.05}$	$1.0^{+0.1}_{-0.2}$	$3.4^{+0.7}_{-1.7}\times10^{56}$	450^{+180}_{-190}	$0.09^{+0.04}_{-0.04}$	1033
GW170104	$30.8^{+7.3}_{-5.6}$	$20.0^{+4.9}_{-4.6}$	$21.4^{+2.2}_{-1.8}$	$-0.04^{+0.17}_{-0.21}$	$48.9^{+5.1}_{-4.0}$	$0.66^{+0.08}_{-0.11}$	$2.2^{+0.5}_{-0.5}$	$3.3^{+0.6}_{-1.0}\times10^{56}$	990^{+440}_{-430}	$0.20^{+0.08}_{-0.08}$	921
GW170608	$11.0^{+5.5}_{-1.7}$	$7.6^{+1.4}_{-2.2}$	$7.9^{+0.2}_{-0.2}$	$0.03^{+0.19}_{-0.07}$	$17.8^{+3.4}_{-0.7}$	$0.69^{+0.04}_{-0.04}$	$0.9^{+0.0}_{-0.1}$	$3.5^{+0.4}_{-1.3}\times10^{56}$	320^{+120}_{-110}	$0.07^{+0.02}_{-0.02}$	392
GW170729	$50.2^{+16.2}_{-10.2}$	$34.0^{+9.1}_{-10.1}$	$35.4^{+6.5}_{-4.8}$	$0.37^{+0.21}_{-0.25}$	$79.5^{+14.7}_{-10.2}$	$0.81^{+0.07}_{-0.13}$	$4.8^{+1.7}_{-1.7}$	$4.2^{+0.9}_{-1.5}\times10^{56}$	2840^{+1400}_{-1360}	$0.49^{+0.19}_{-0.21}$	1041
GW170809	$35.0^{+8.3}_{-5.9}$	$23.8^{+5.1}_{-5.2}$	$24.9^{+2.1}_{-1.7}$	$0.08^{+0.17}_{-0.17}$	$56.3^{+5.2}_{-3.8}$	$0.70^{+0.08}_{-0.09}$	$2.7^{+0.6}_{-0.6}$	$3.5^{+0.6}_{-0.9}\times10^{56}$	1030^{+320}_{-390}	$0.20^{+0.05}_{-0.07}$	308
GW170814	$30.6^{+5.6}_{-3.0}$	$25.2^{+2.8}_{-4.0}$	$24.1^{+1.4}_{-1.1}$	$0.07^{+0.12}_{-0.12}$	$53.2^{+3.2}_{-2.4}$	$0.72^{+0.07}_{-0.05}$	$2.7^{+0.4}_{-0.3}$	$3.7^{+0.4}_{-0.5}\times10^{56}$	600^{+150}_{-220}	$0.12^{+0.03}_{-0.04}$	87
GW170817	$1.46^{+0.12}_{-0.10}$	$1.27^{+0.09}_{-0.09}$	$1.186^{+0.001}_{-0.001}$	$0.00^{+0.02}_{-0.01}$	≤ 2.8	≤ 0.89	≥ 0.04	$\geq 0.1\times10^{56}$	40^{+7}_{-15}	$0.01^{+0.00}_{-0.00}$	16
GW170818	$35.4^{+7.5}_{-4.7}$	$26.7^{+4.3}_{-5.2}$	$26.5^{+2.1}_{-1.7}$	$-0.09^{+0.18}_{-0.21}$	$59.4^{+4.9}_{-3.8}$	$0.67^{+0.07}_{-0.08}$	$2.7^{+0.5}_{-0.5}$	$3.4^{+0.5}_{-0.7}\times10^{56}$	1060^{+420}_{-380}	$0.21^{+0.07}_{-0.07}$	39
GW170823	$39.5^{+11.2}_{-6.7}$	$29.0^{+6.7}_{-7.8}$	$29.2^{+4.6}_{-3.6}$	$0.09^{+0.22}_{-0.26}$	$65.4^{+10.1}_{-7.4}$	$0.72^{+0.09}_{-0.12}$	$3.3^{+1.0}_{-0.9}$	$3.6^{+0.7}_{-1.1}\times10^{56}$	1940^{+970}_{-900}	$0.35^{+0.15}_{-0.15}$	1666

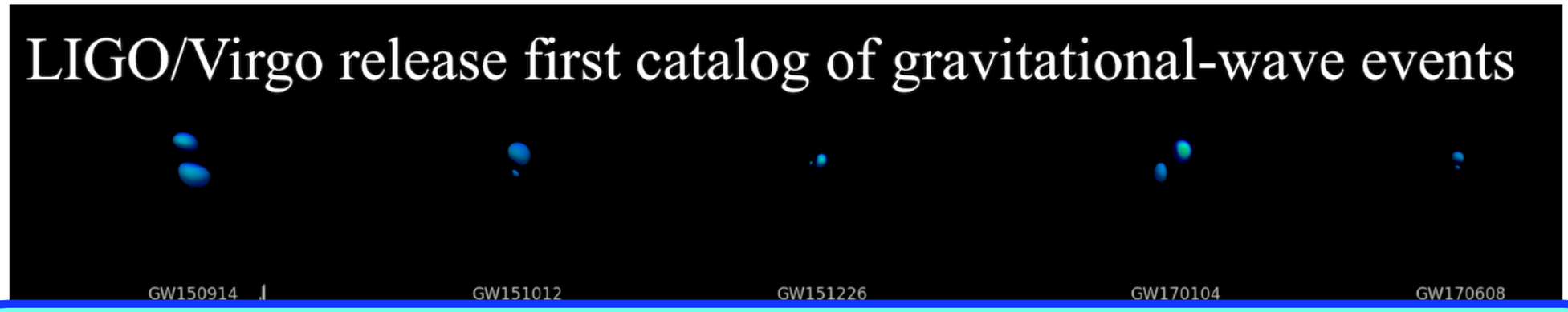

> 33 (and counting) compact binary merger candidates in O3!

Maximum distance observed approx. 4 Gpc

Even											/deg^2
GW1											82
GW1											523
GW1											033
GW1											921
GW1											392
GW1											1041
GW170809	$35.0^{+8.3}_{-5.9}$	$23.8^{+5.1}_{-5.2}$	$24.9^{+2.1}_{-1.7}$	$0.08^{+0.17}_{-0.17}$	$56.3^{+5.2}_{-3.8}$	$0.70^{+0.08}_{-0.09}$	$2.7^{+0.6}_{-0.6}$	$3.5^{+0.6}_{-0.9} \times 10^{56}$	1030^{+320}_{-390}	$0.20^{+0.05}_{-0.07}$	308
GW170814	$30.6^{+5.6}_{-3.0}$	$25.2^{+2.8}_{-4.0}$	$24.1^{+1.4}_{-1.1}$	$0.07^{+0.12}_{-0.12}$	$53.2^{+3.2}_{-2.4}$	$0.72^{+0.07}_{-0.05}$	$2.7^{+0.4}_{-0.3}$	$3.7^{+0.4}_{-0.5} \times 10^{56}$	600^{+150}_{-220}	$0.12^{+0.03}_{-0.04}$	87
GW170817	$1.46^{+0.12}_{-0.10}$	$1.27^{+0.09}_{-0.09}$	$1.186^{+0.001}_{-0.001}$	$0.00^{+0.02}_{-0.01}$	≤ 2.8	≤ 0.89	≥ 0.04	$\geq 0.1 \times 10^{56}$	40^{+7}_{-15}	$0.01^{+0.00}_{-0.00}$	16
GW170818	$35.4^{+7.5}_{-4.7}$	$26.7^{+4.3}_{-5.2}$	$26.5^{+2.1}_{-1.7}$	$-0.09^{+0.18}_{-0.21}$	$59.4^{+4.9}_{-3.8}$	$0.67^{+0.07}_{-0.08}$	$2.7^{+0.5}_{-0.5}$	$3.4^{+0.5}_{-0.7} \times 10^{56}$	1060^{+420}_{-380}	$0.21^{+0.07}_{-0.07}$	39
GW170823	$39.5^{+11.2}_{-6.7}$	$29.0^{+6.7}_{-7.8}$	$29.2^{+4.6}_{-3.6}$	$0.09^{+0.22}_{-0.26}$	$65.4^{+10.1}_{-7.4}$	$0.72^{+0.09}_{-0.12}$	$3.3^{+1.0}_{-0.9}$	$3.6^{+0.7}_{-1.1} \times 10^{56}$	1940^{+970}_{-900}	$0.35^{+0.15}_{-0.15}$	1666

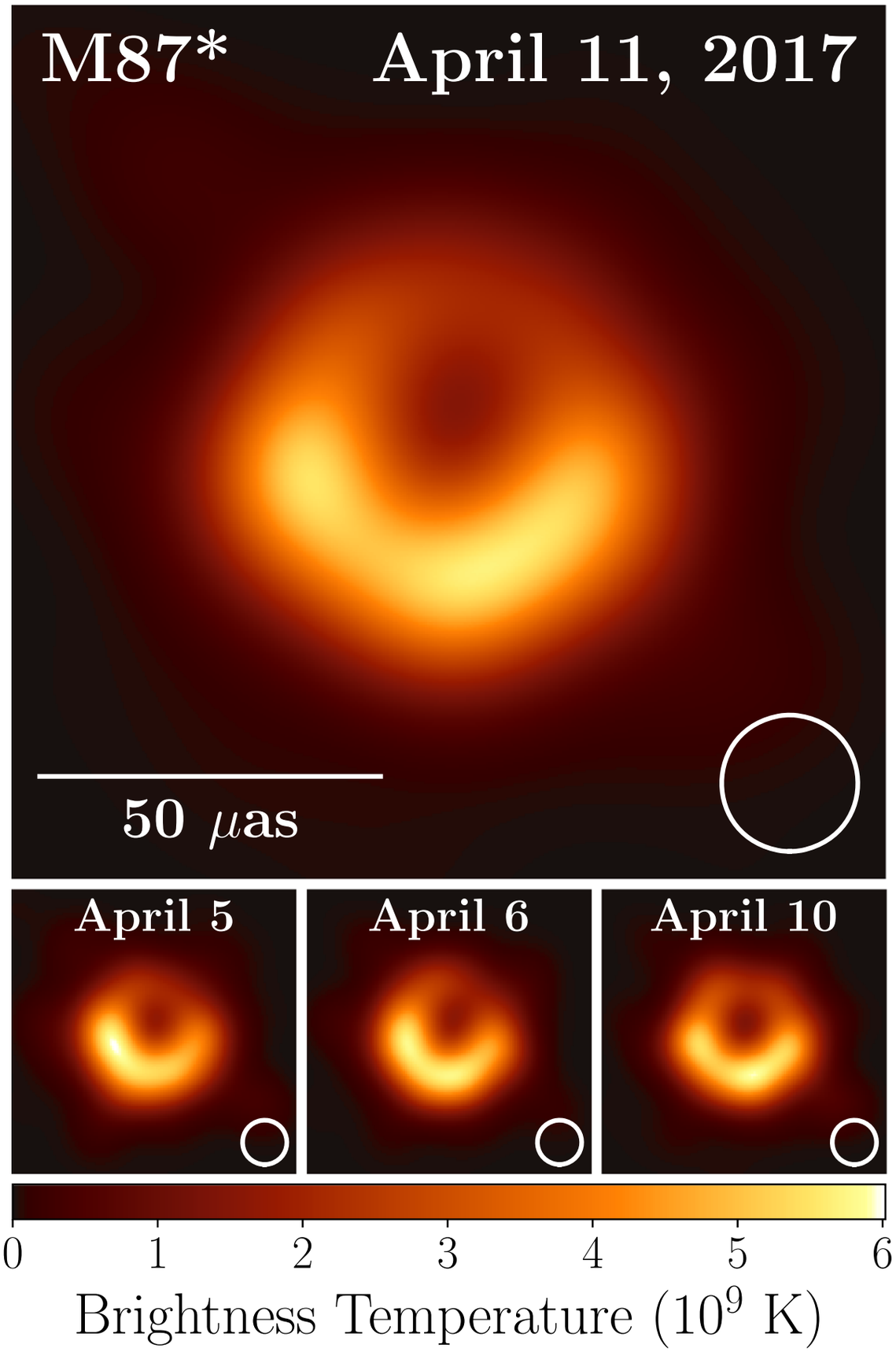

First image of the “shadow” of a supermassive black hole

A visual evidence: the image of the center of the M87 galaxy recorded with the Event Horizon Telescope (EHT).

From The EHT collaboration et al., 2019, ApJ, 875, L1.

Indirect (but quite compelling) evidence of GW emission is known for 4 decades from radio observations of binary pulsars (compact relativistic binaries)

PSR 1913+16: Hulse & Taylor (1975) [double neutron star binary]

PSR J0348+0432: Antoniadis et al. (2013) [neutron star - white dwarf binary]

Show decay in orbital period decay according to GR

$$\left\langle \frac{da}{dt} \right\rangle = -\frac{64G^3}{5c^5} m_1 m_2 (m_1 + m_2) a^{-3} (1 - e^2)^{-\frac{7}{2}}$$

$$\tau_{\rm mrg} \approx \frac{5}{64} \frac{c^5 a^4 (1 - e^2)^{7/2}}{G^3 m_1 m_2 (m_1 + m_2)} \left(1 + \frac{73}{24} e^2 + \frac{37}{96} e^4\right)^{-1}$$

Peters (1964)

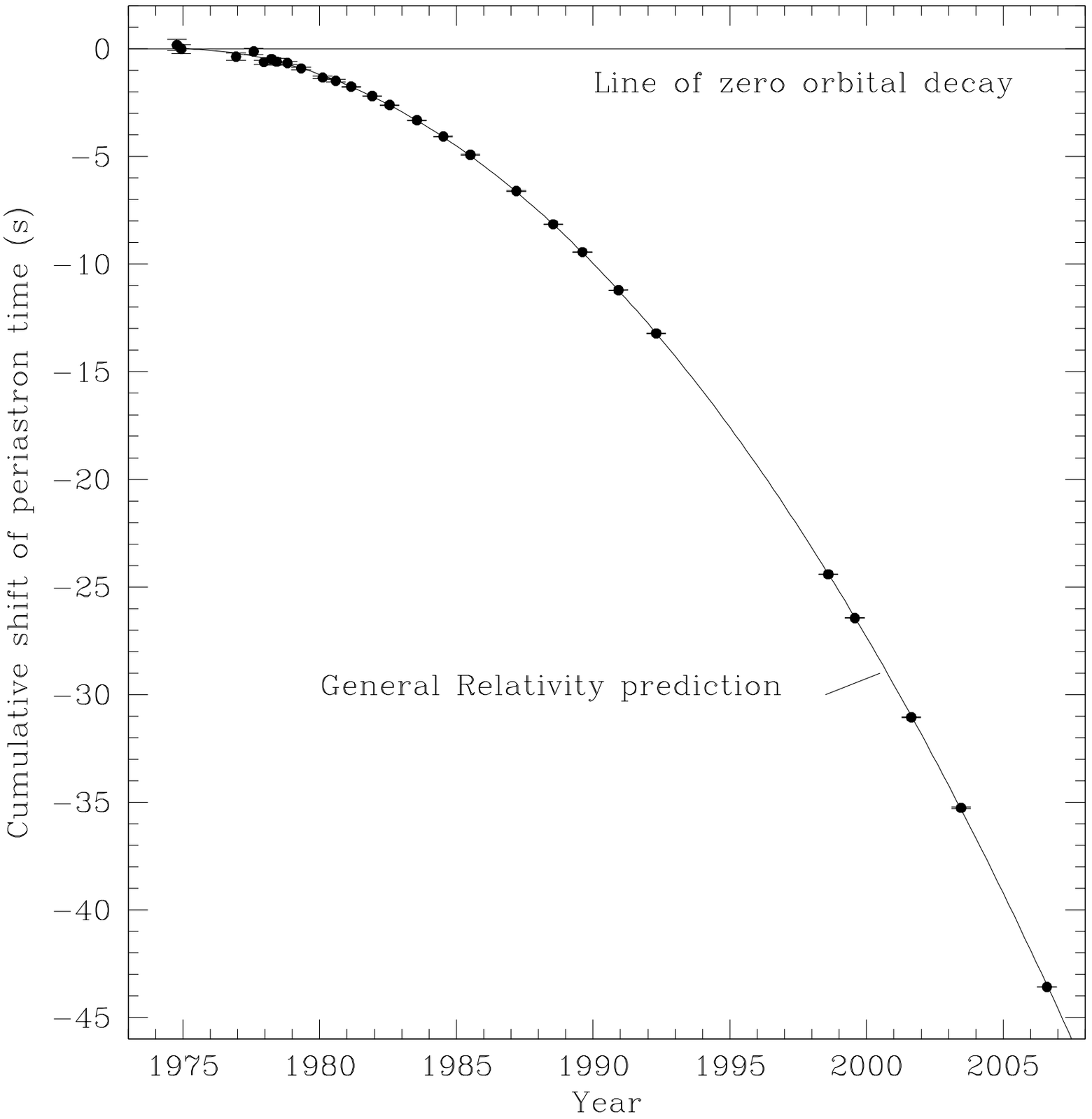

PSR 1913+16: Weisberg et al. (2010)

Sources of gravitational waves

- Binary BH - strongest source of GW. GW emission until "as close as two masses can get". In-spirals of stellar and supermassive BHs.

- Other compact binaries: BH-NS, NS-NS, WD-WD. BH-NS and NS-NS binaries can produce short GRBs too.

- Surface anomalies on rapidly spinning neutron stars, neutron star glitches

- Supernovae

- Primordial (cosmic) GW background

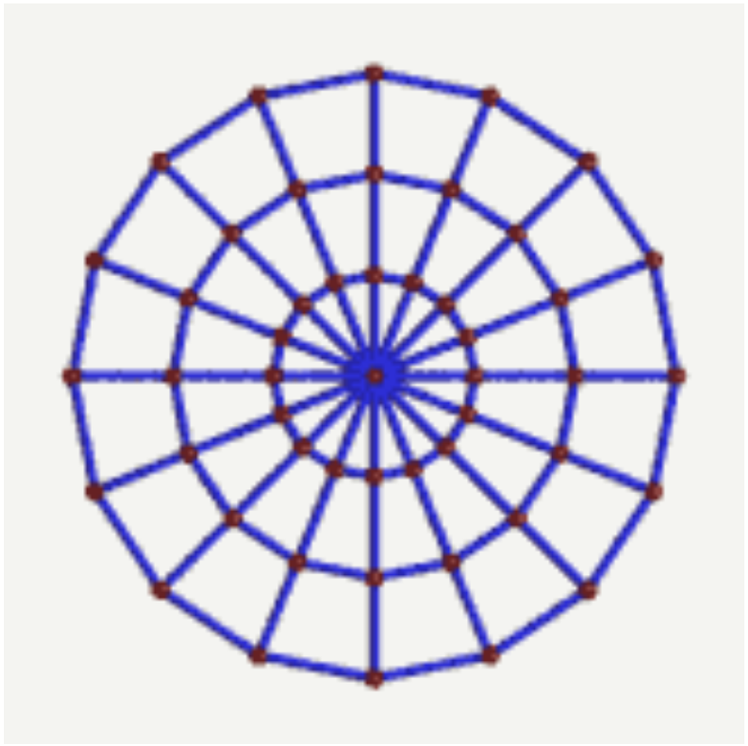

Animation credit: AEI/Einstein online

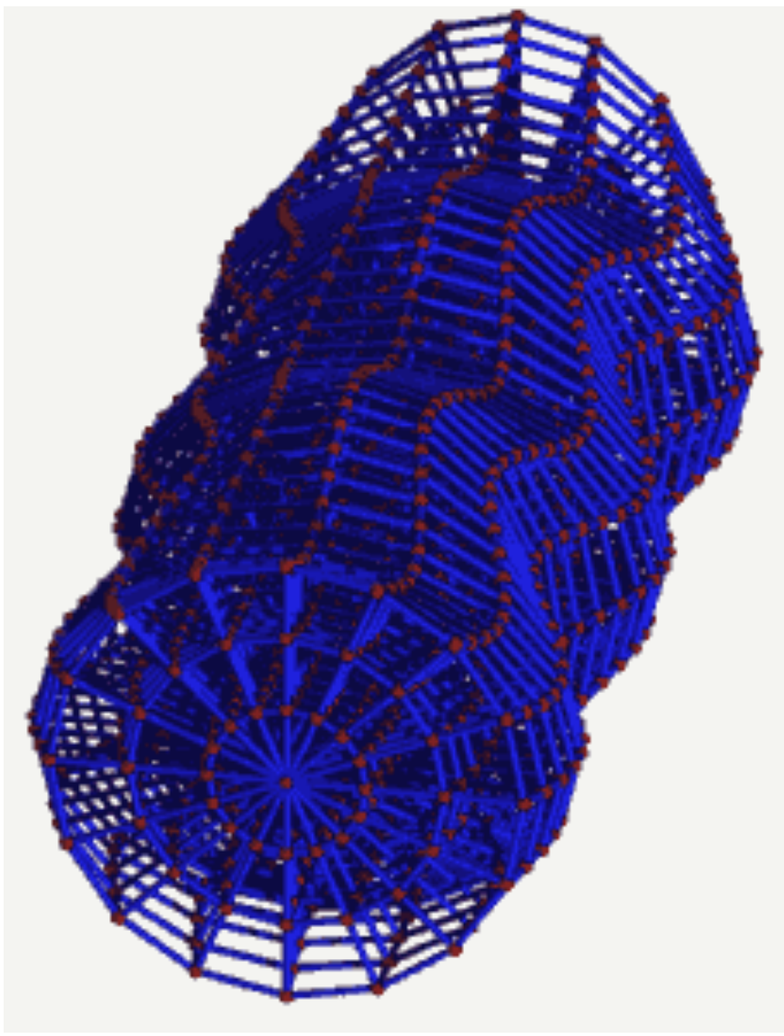

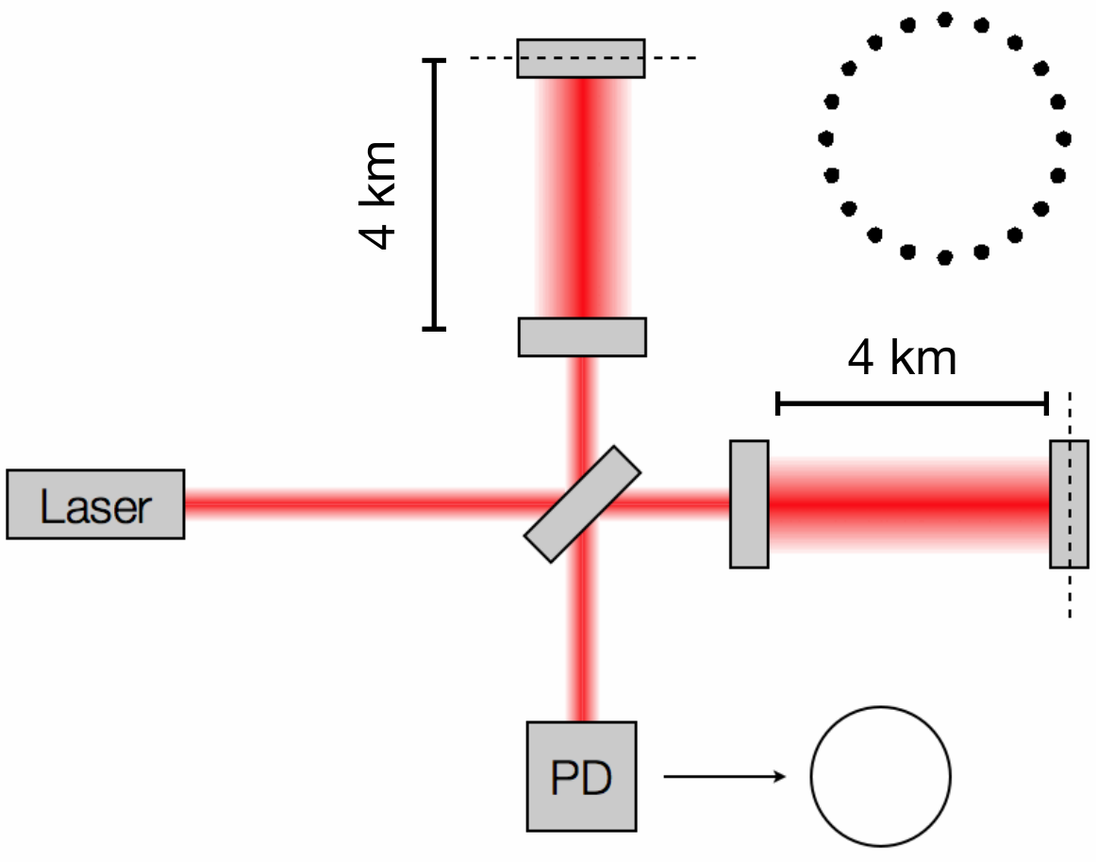

Animation credit: Penn State University

For LIGO-Virgo (3-4 km arm):

Actual mirror displacement:
~1/1000 th of the proton's diameter

High-frequency detector:
10 Hz - 1000 Hz (most sensitive at ~100 Hz)

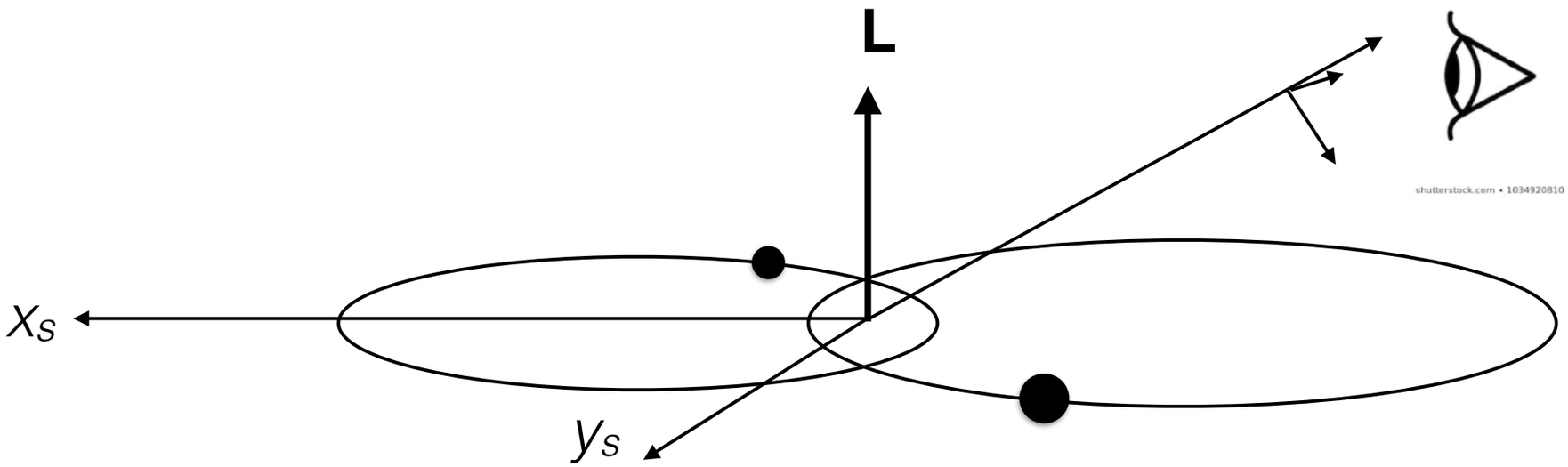

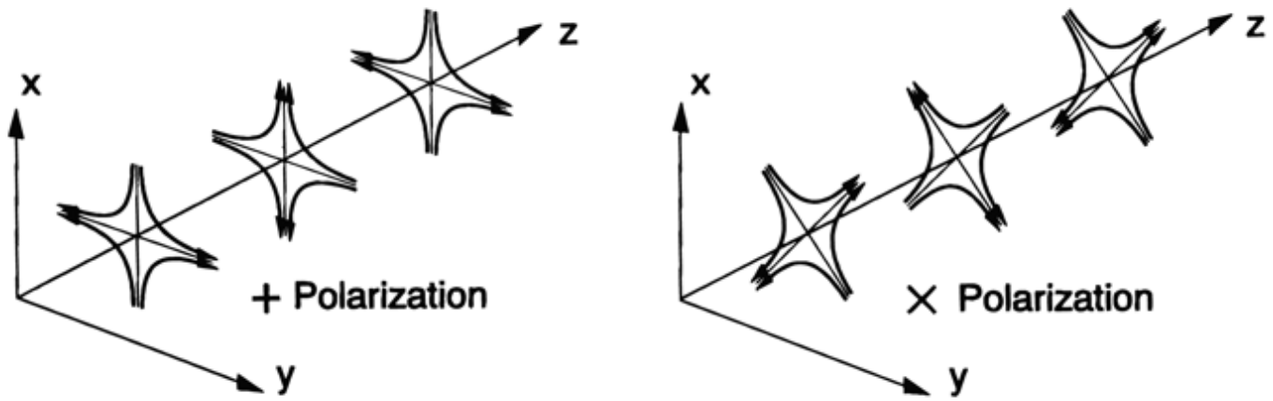

GW from a binary is polarized

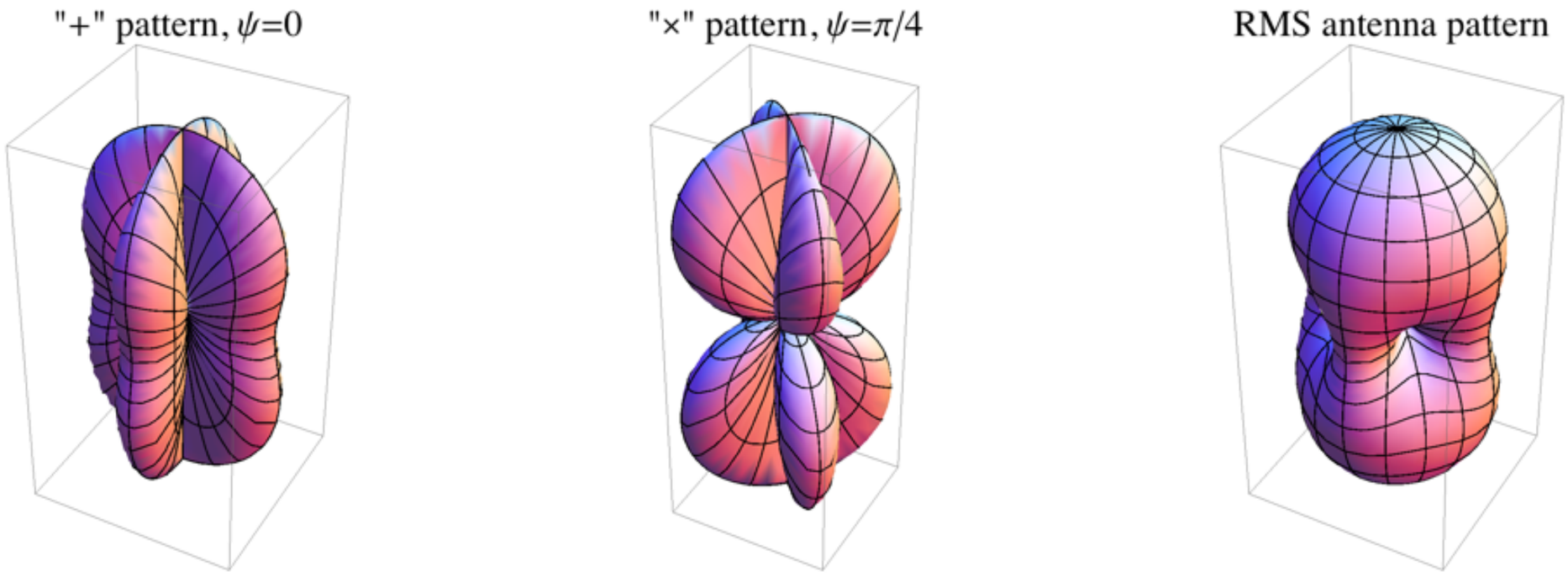

Image credit: Matt Benacquista

(Advanced) Laser Interferometer Gravitational Observatory (LIGO) at Hanford (also in Livingston and Pisa [Virgo])

(evolving) Laser Interferometer Space Antenna (eLISA)

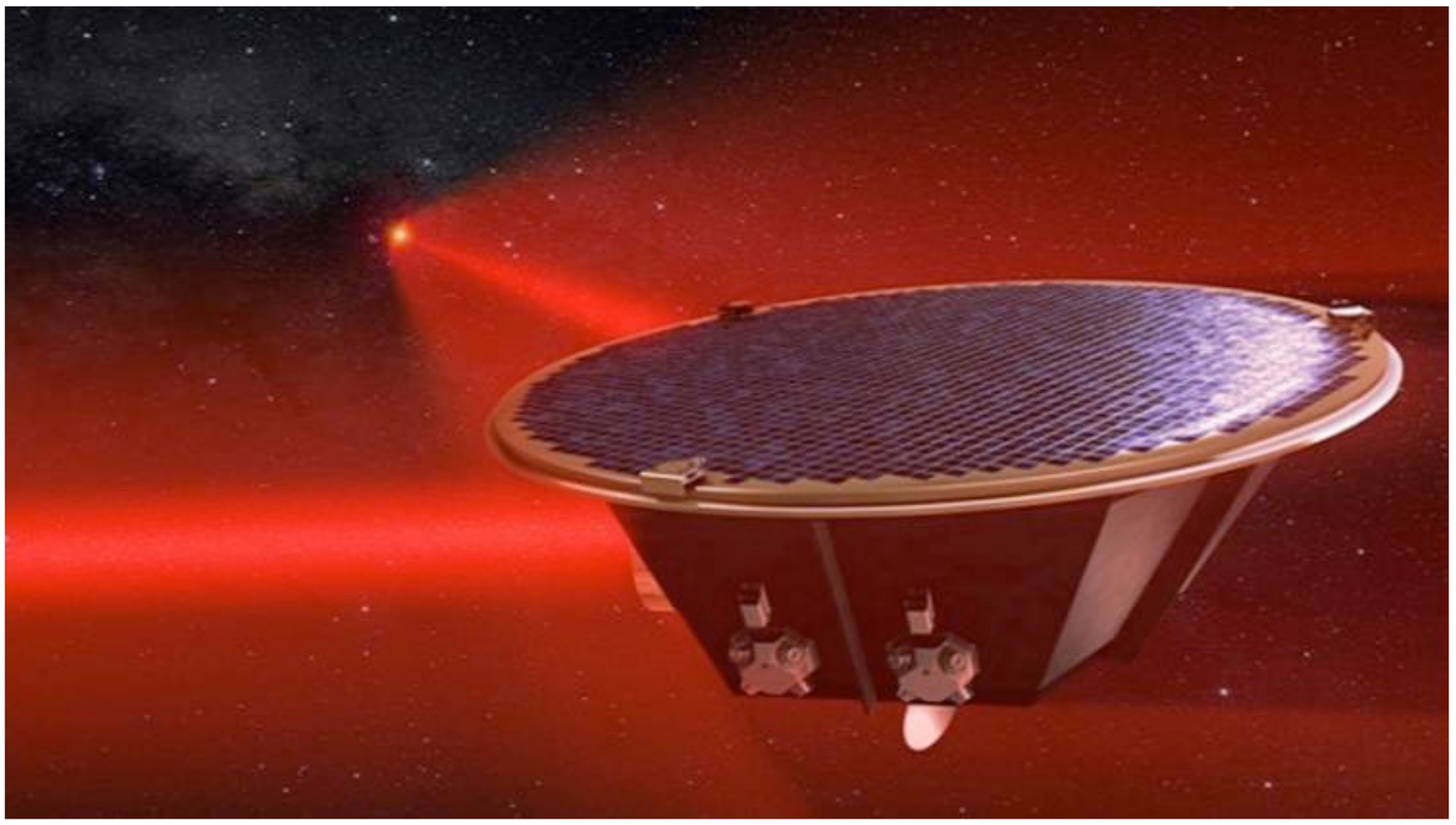

Stellar black hole and neutron star binary inspirals

Neutron star surface anomalies and glitches

Core-collapse supernovae

Binary supermassive black hole inspirals

IMBH inspirals

Binary stellar black holes

Binary white dwarfs

Primordial GW

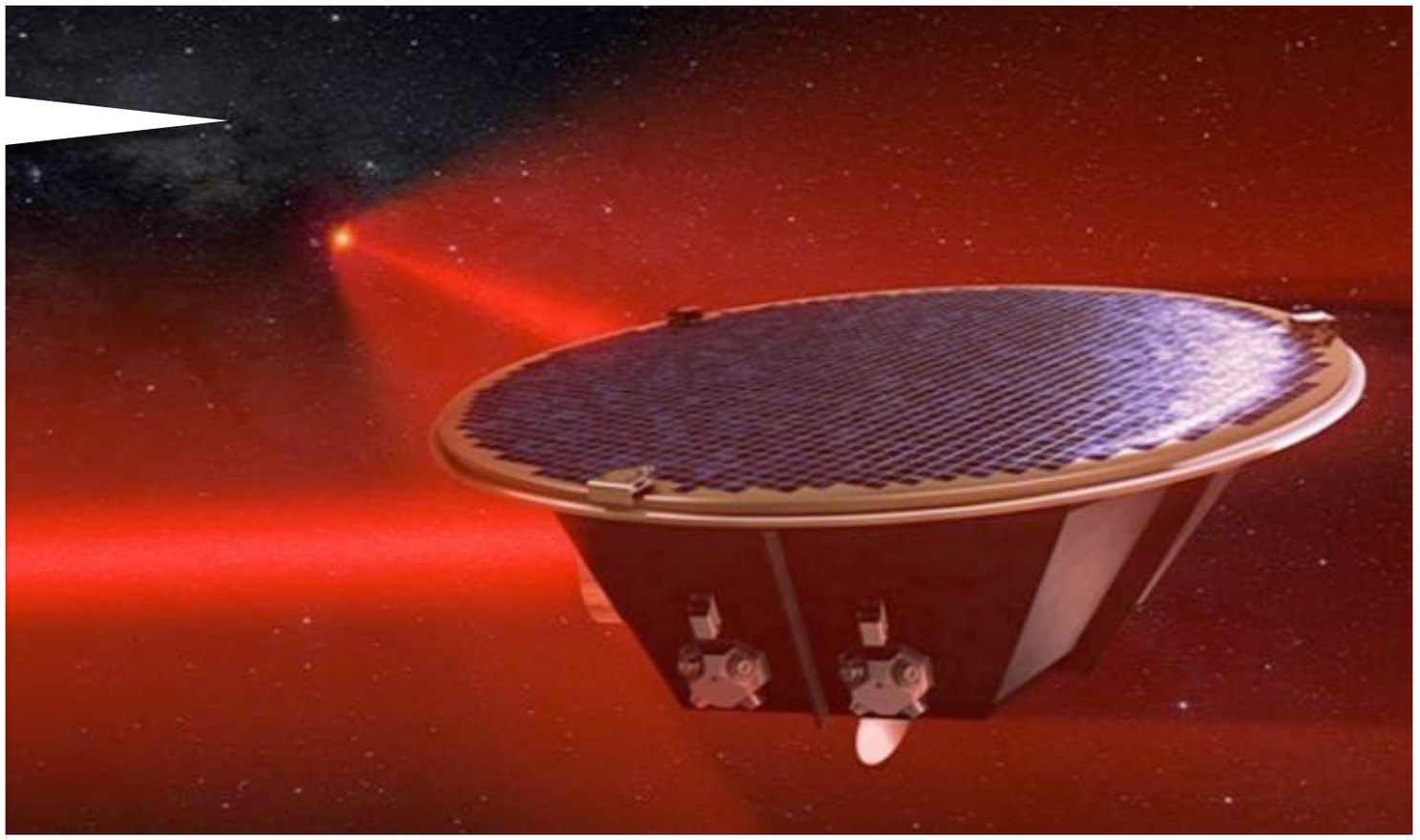

Pulsar timing arrays (PTA)

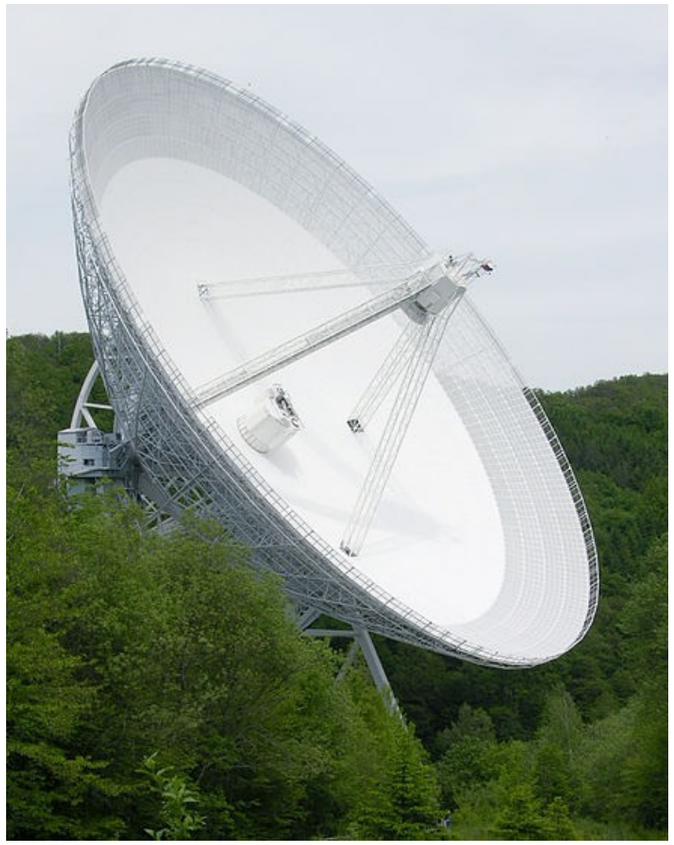

Effelsberg radio telescope

Parkes radio telescope

GW detection from correlations in pulse arrival times from an array of pulsars

Binary supermassive BH, GW background

Pulsar timing arrays (PTA)

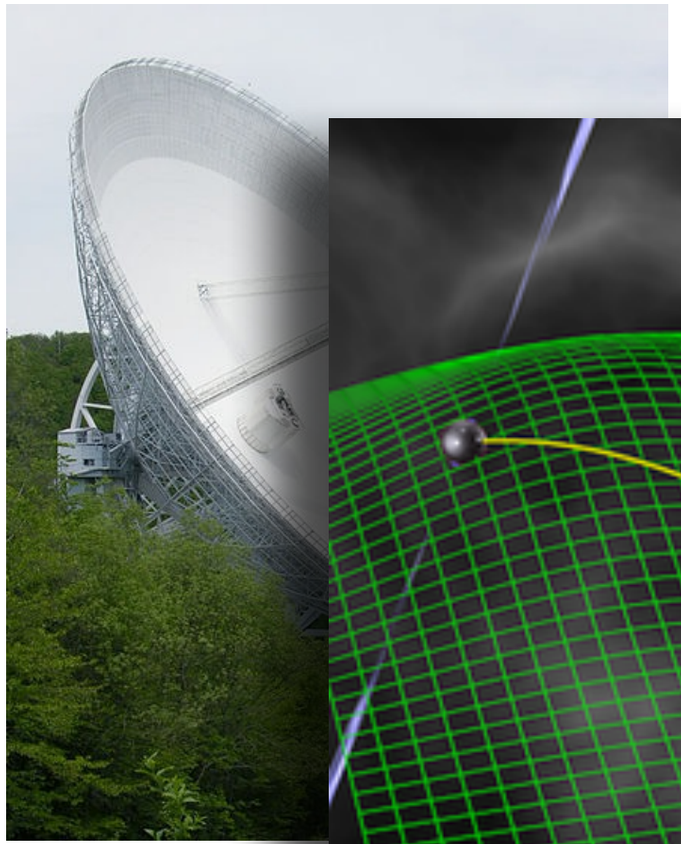

Effelsberg ra

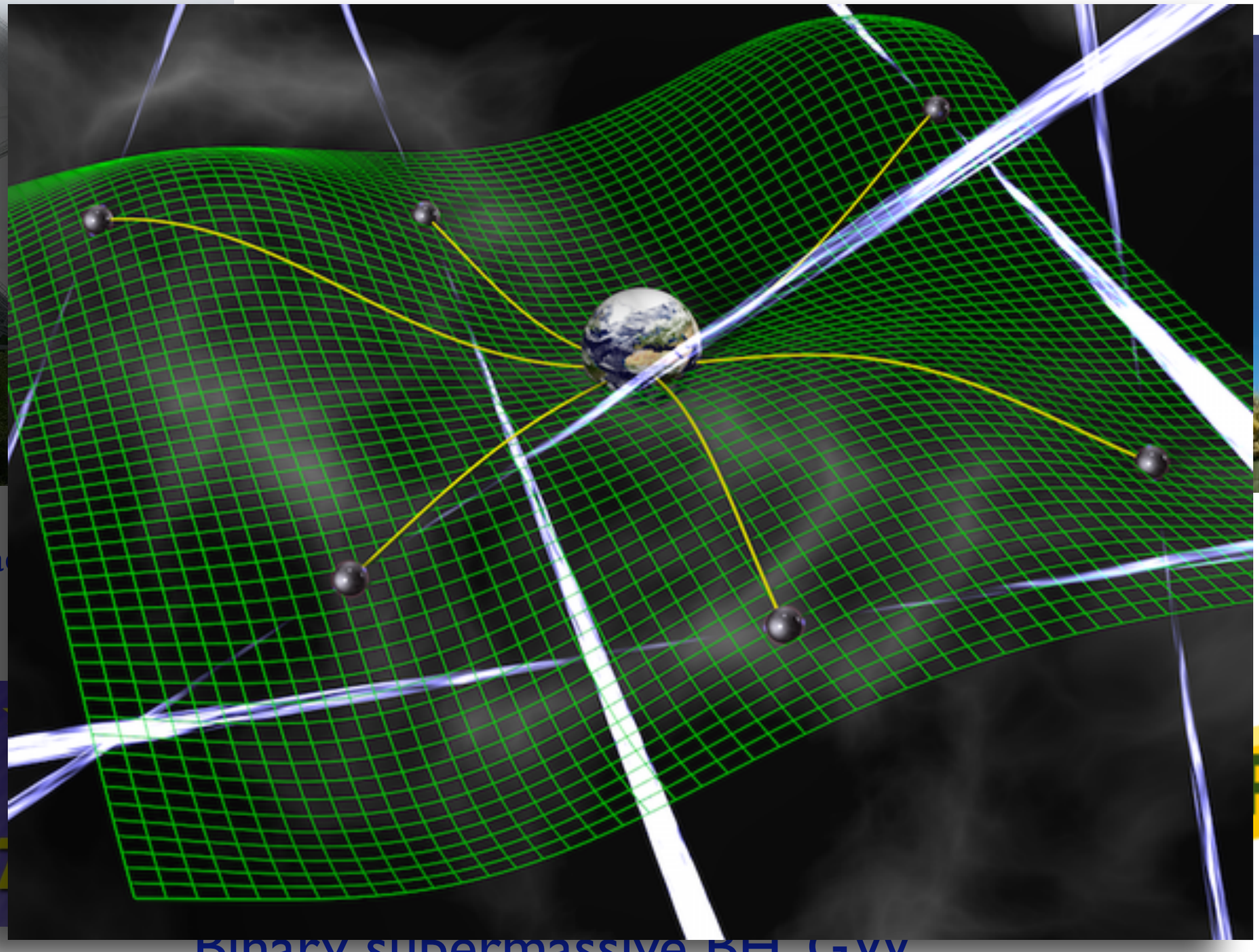

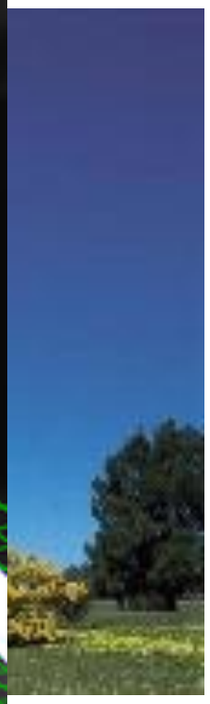

EP

PTA

Binary supermassive BH, GW background

Pulsar timing arrays (PTA)

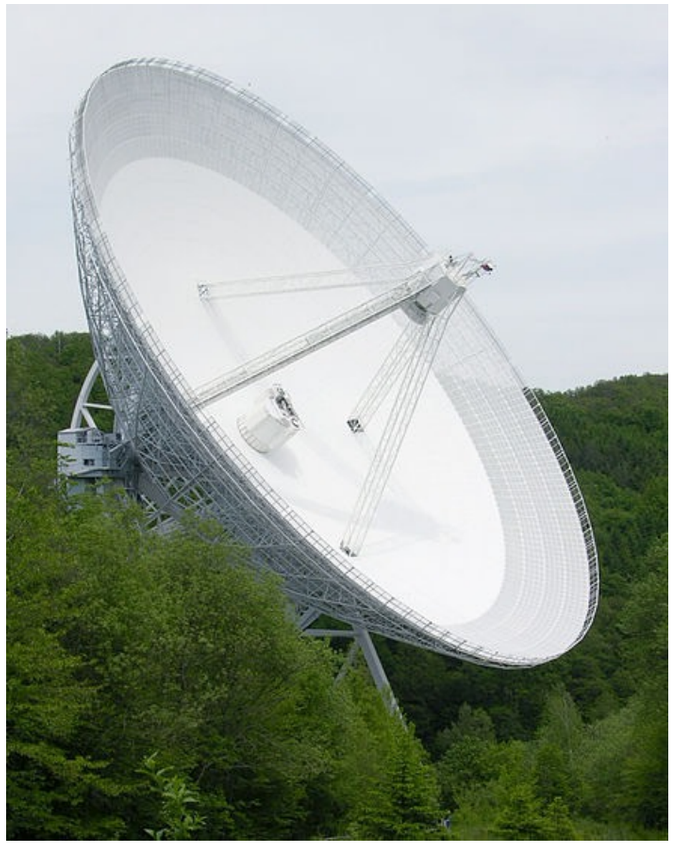

Effelsberg radio telescope

Parkes radio telescope

GW detection from correlations in pulse arrival times from an array of pulsars

Binary supermassive BH, GW background

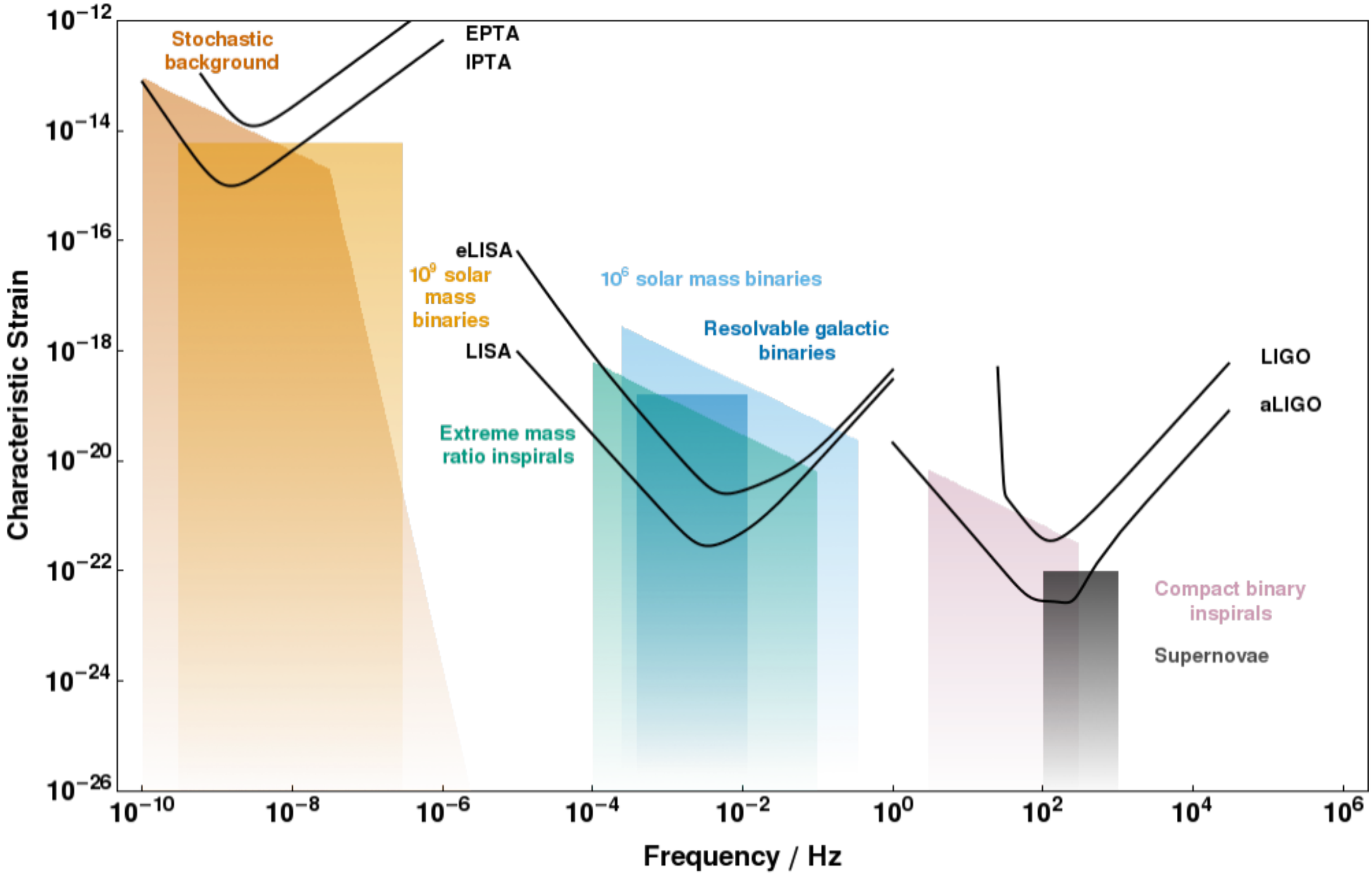

Credit: Christopher Moore, Robert Cole and Christopher Berry (IoA Cambridge)

GW frequency from a binary (Wen 2003)

$$f_{\mathrm{GWp}} = \frac{\sqrt{G(m_1+m_2)}}{\pi}\,\frac{(1+e)^{1.1954}}{\left[a(1-e^2)\right]^{1.5}}$$

GW from an eccentric binary is polychromatic. f_{GWp} represents the frequency with the peak GW power.

[Note the strong eccentricity dependence!]

Chirp mass

$$M_{\mathrm{chirp}} \equiv \frac{(m_1 m_2)^{3/5}}{(m_1+m_2)^{1/5}}$$

$$= \frac{c^3}{G}\left[\frac{5}{96}\pi^{-8/3} f^{-11/3}\dot{f}\right]^{3/5}$$

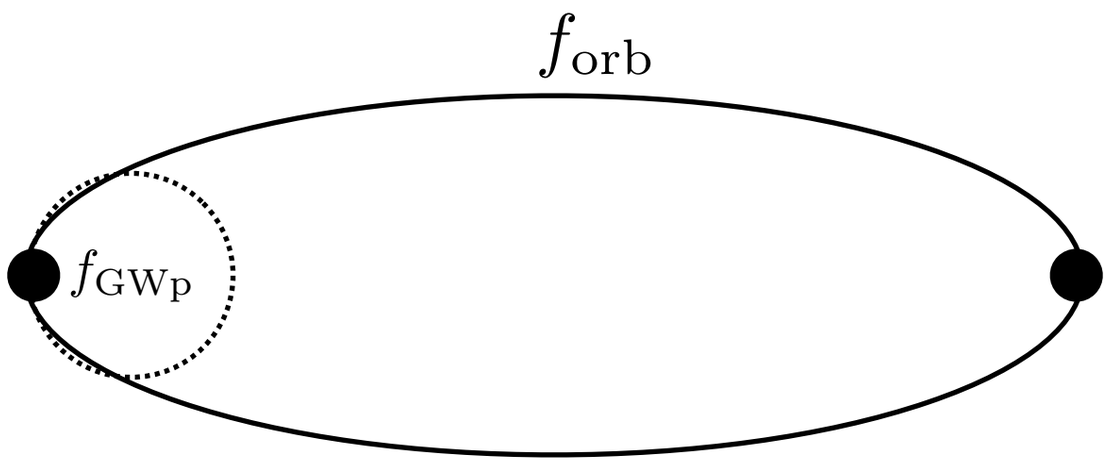

GW chirp for circular binaries
L. Blanchet et al., Phys. Rev. Lett. 74, 3515 (1995)

Kamioka Gravitational Wave Detector (KAGRA)

3km-arm interferometer

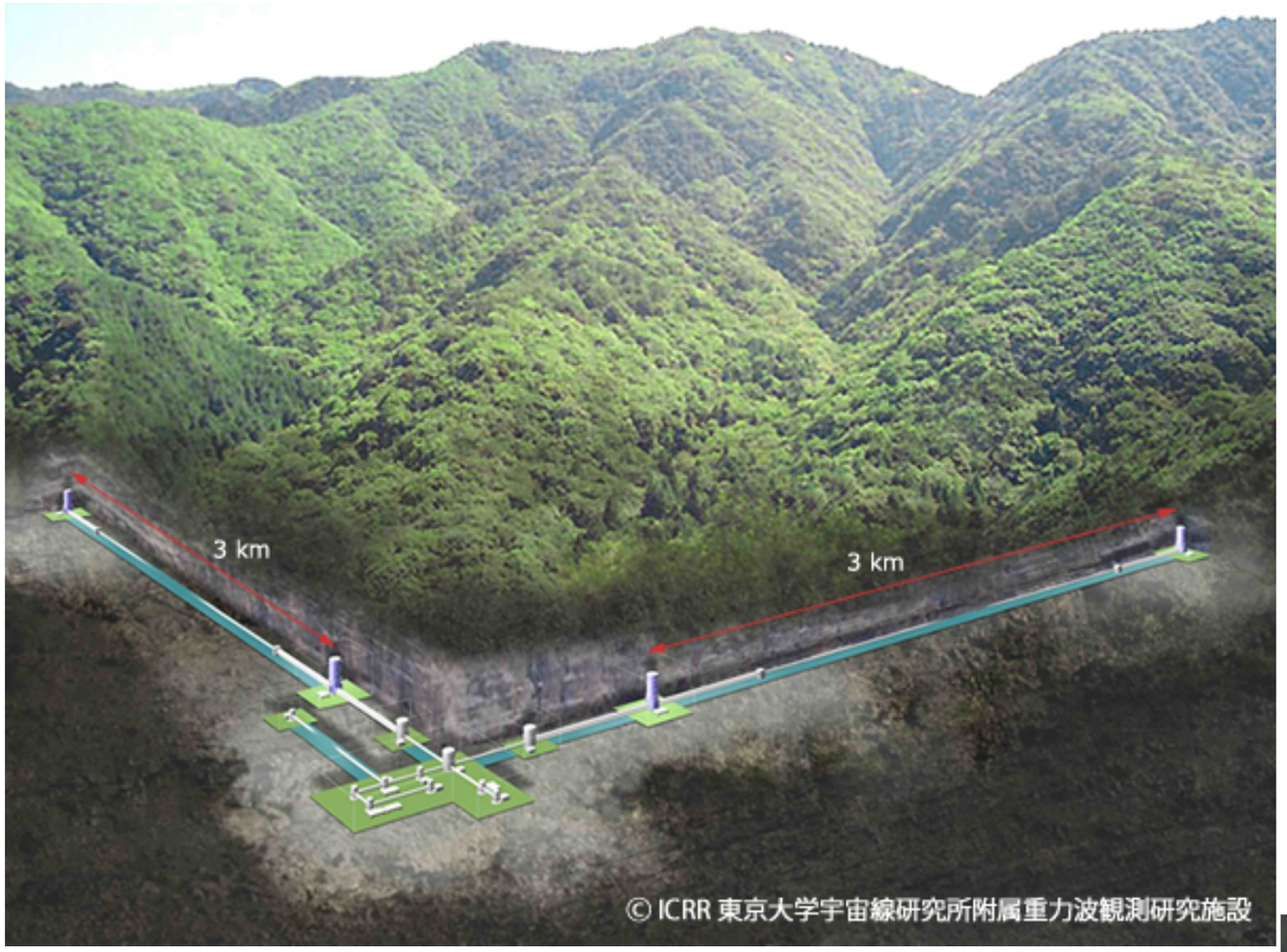

~ 2019

LIGO-India/IndIGO: 4 km-arm interferometer. In-principle approval from Indian government. Target: ~ 2024

Einstein Telescope: 3-arm interferometer, each 10 km long. Low- and high-frequency bands. Concept stage.

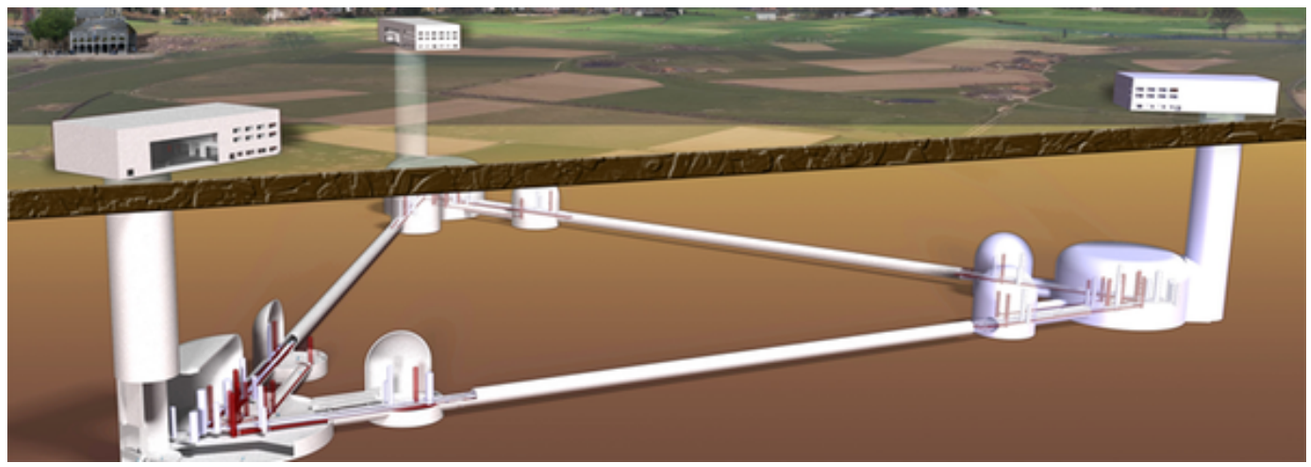

Stellar mass black holes in star clusters

60 lightyear (20 parsec)

47 Tuc (credit NASA/ESA/HST)

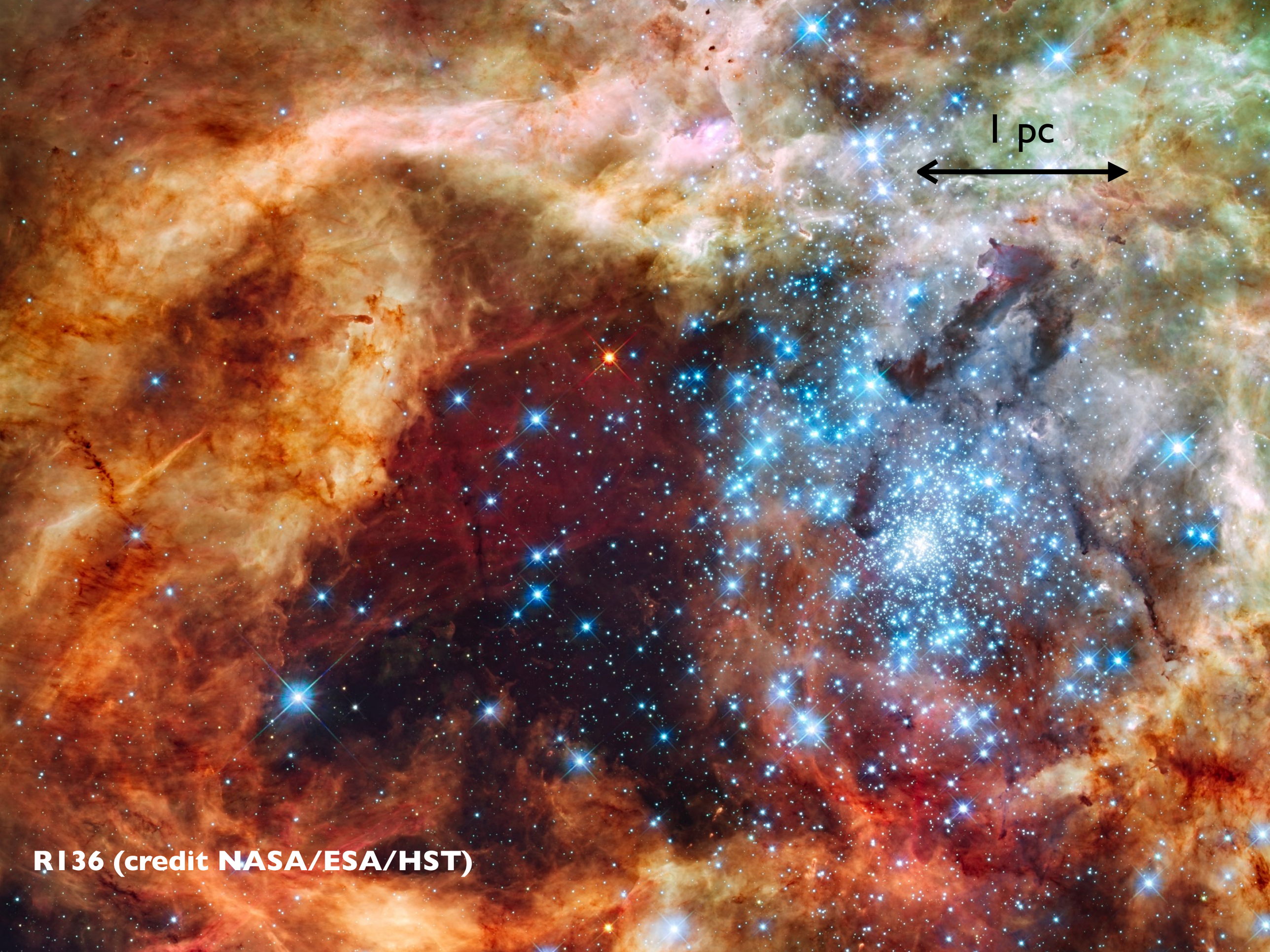
1 pc
R136 (credit NASA/ESA/HST)

Zero-age main sequence (ZAMS) mass $\gtrsim 8M_\odot$

NS

Mass $\approx 1.4M_\odot$ (Chandrasekhar limit) – $\approx 3M_\odot$

Radius ~ 10 Km

Maximum mass & radius depends on equation of state (EOS) of matter at nuclear density

Zero-age main sequence (ZAMS) mass $\gtrsim 18M_\odot$

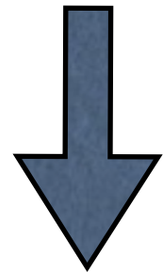

BH

mass depends on (a) stellar metallicity Z (b) nature of stellar wind [(c) supernova characteristics]

average mass $\approx 10M_\odot$ (low$Z$), maximum measured mass so far $\approx 30M_\odot$ (IC10 SFR)

Radius = event-horizon =

$$\frac{r_s + \sqrt{r_s^2 - 4\alpha^2}}{2},$$

$$r_s = 2GM/c^2, \quad \alpha = J/Mc$$

Massive stars (ZAMS mass $\gtrsim 18 M_\odot$) evolve in clusters to produce stellar BHs. BH mass function depends on cluster initial mass function (IMF) and metallicity.

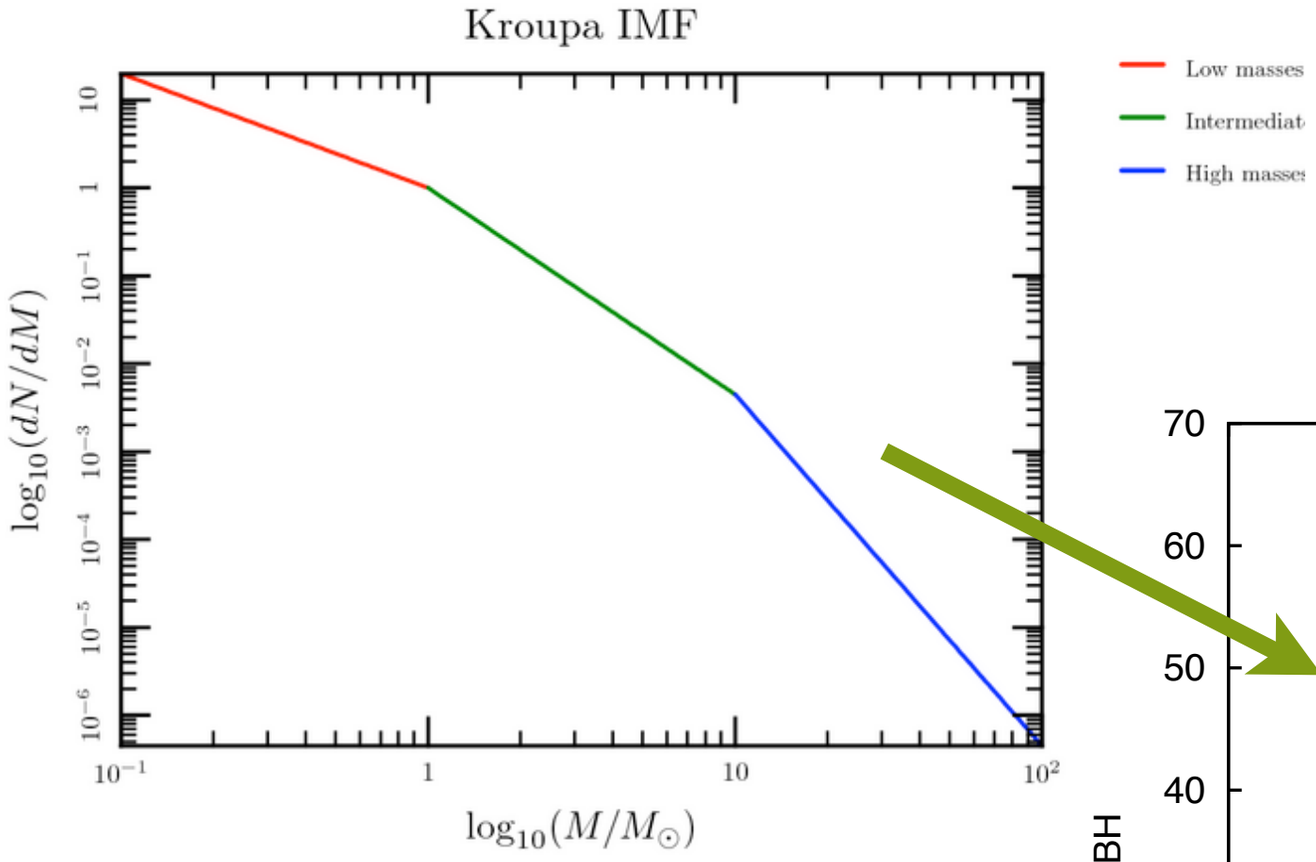

Cluster IMF; Kroupa (2001)

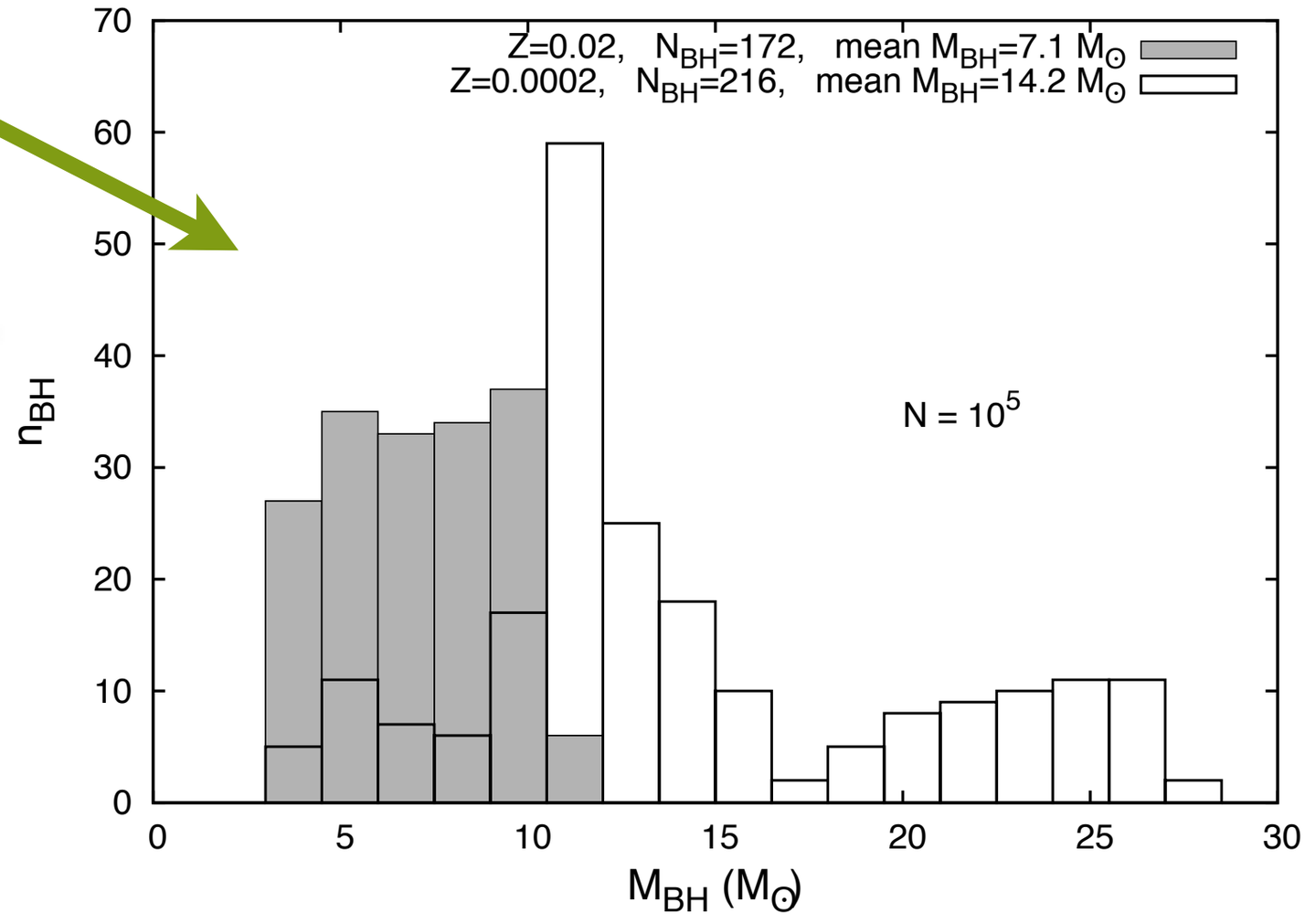

BH mass function

What happens to these newly formed NSs and BHs ?

- Compact remnants (NS/BH) can receive birth / *"natal" velocity kick* due to asymmetry in high-velocity supernova ejecta which carries net momentum.

- The observed average natal kick of field NSs is $\approx 265\ \mathrm{km\ s^{-1}}$

- Amount of kick for BH uncertain (in theory & observation).

- Can be observationally inferred from "back-tracing" orbital motion of Galactic BH X-ray binaries [e.g. ,Willems et al., 2005, ApJ, 625, 324, Repetto et al. 2012] --- indicate *very low to high natal kicks*.

- Computations of core-collapse supernova also support a wide range of natal kicks (Janka et al.).

- BH natal kicks controlled by "material fallback" and SN core size. Stars $\gtrsim 50 M_\odot$ collapse directly to a BH with no or small kicks.

- "Electron Capture" mechanism produces NSs with small kick velocities.

More on lecture 3!

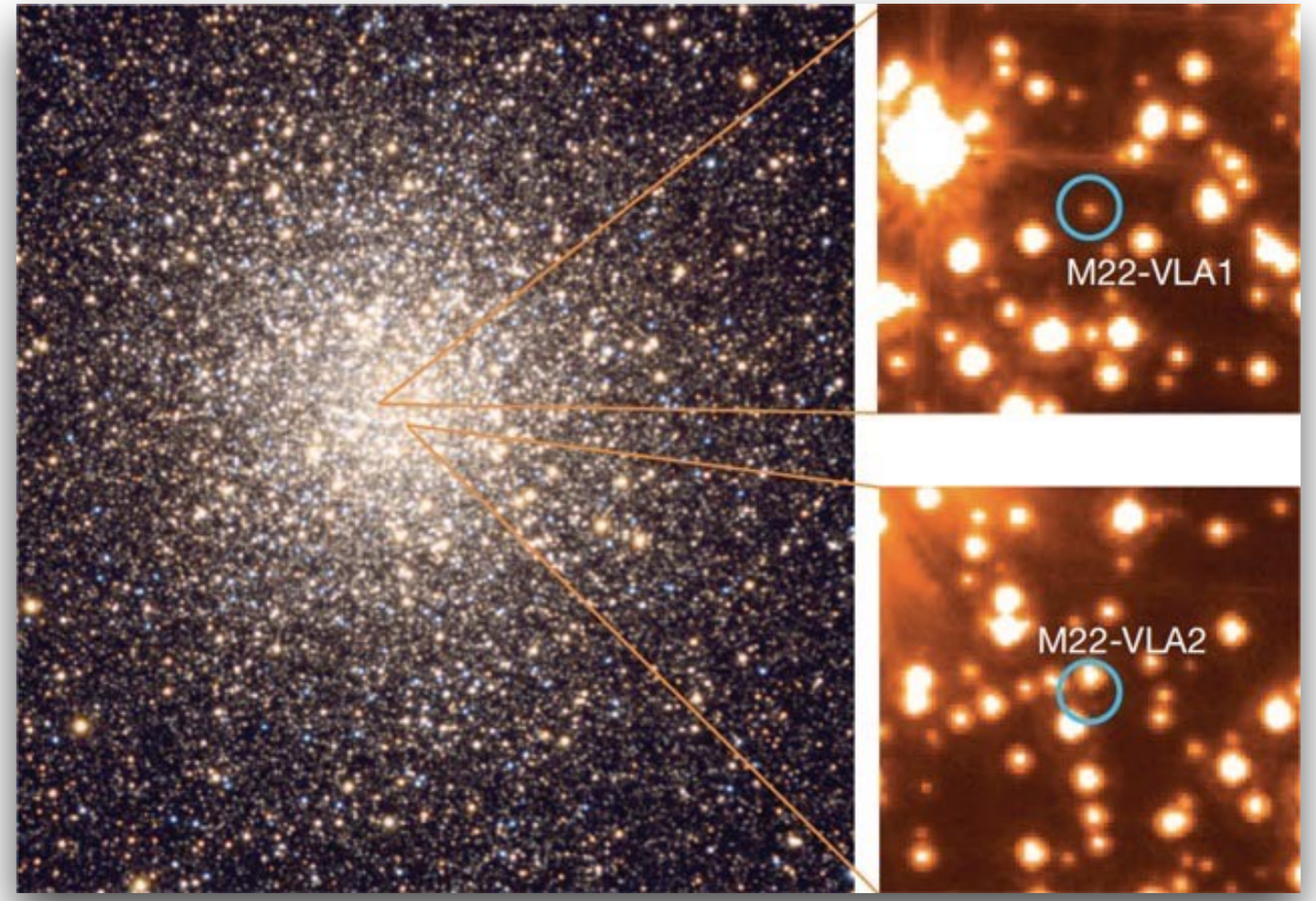

M22 BH candidates (Strader et al. 2012)

Promising source for LIGO-VIRGO gravitational-wave detector

… as well for LISA

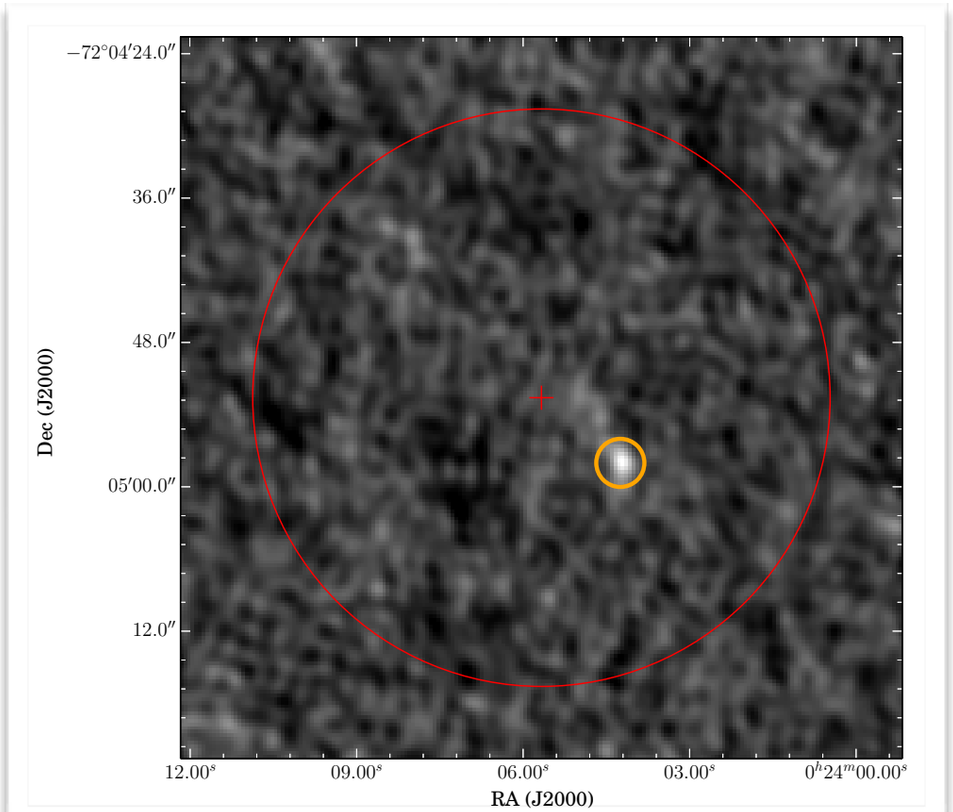

Stellar-mass black holes candidates in globular clusters identified in X-ray and radio

5.5-Ghz image of 47 Tuc core (Miller-Jones et al. 2015)

Also in M62 (Chomiuk et al. 2013); M10 (Shishkovsky et al. 2018)

Accreting BHs are also bright radio sources: radio waves produced by synchrotron emission in jets.

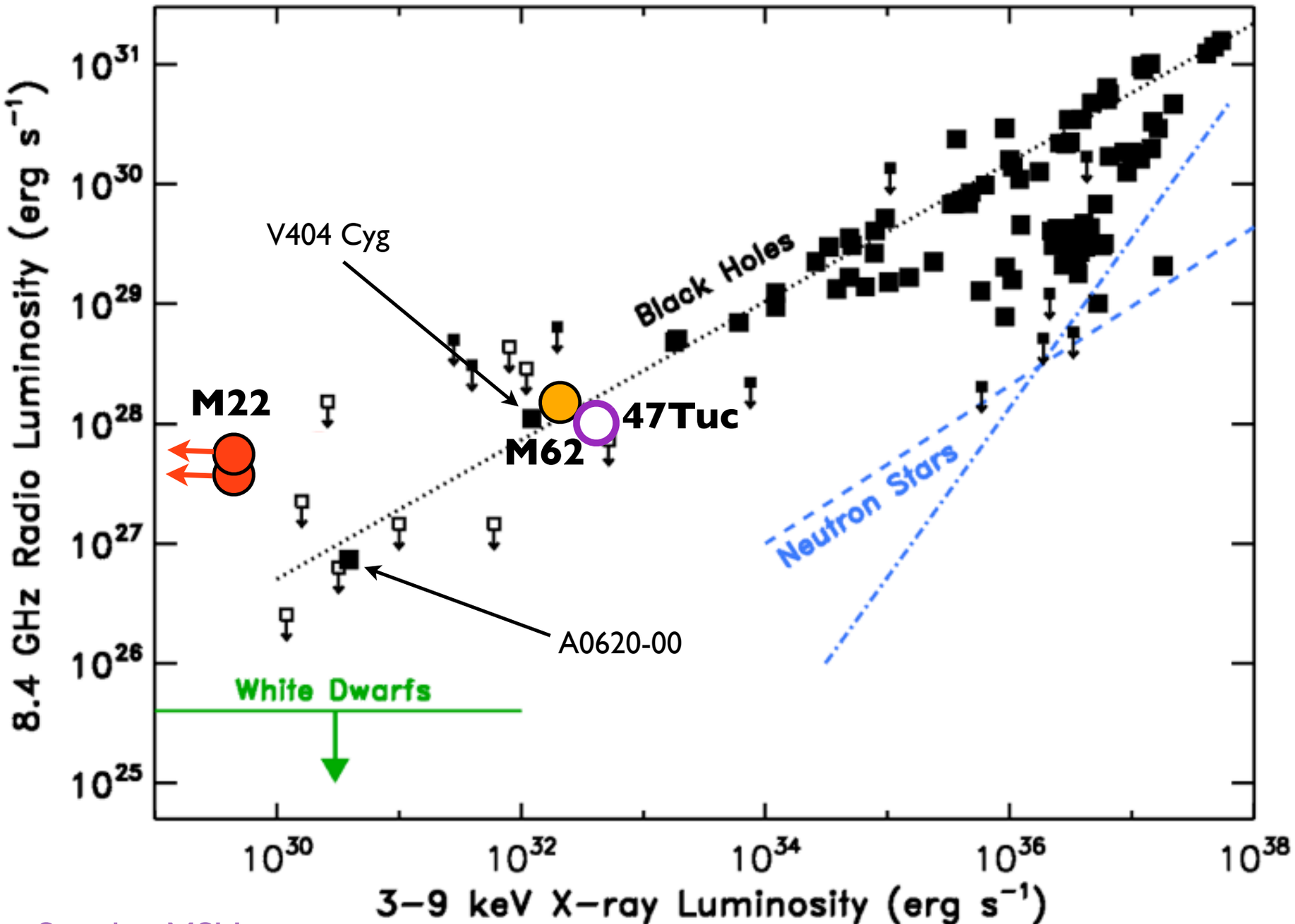

Fig. credit: Jay Strader, MSU

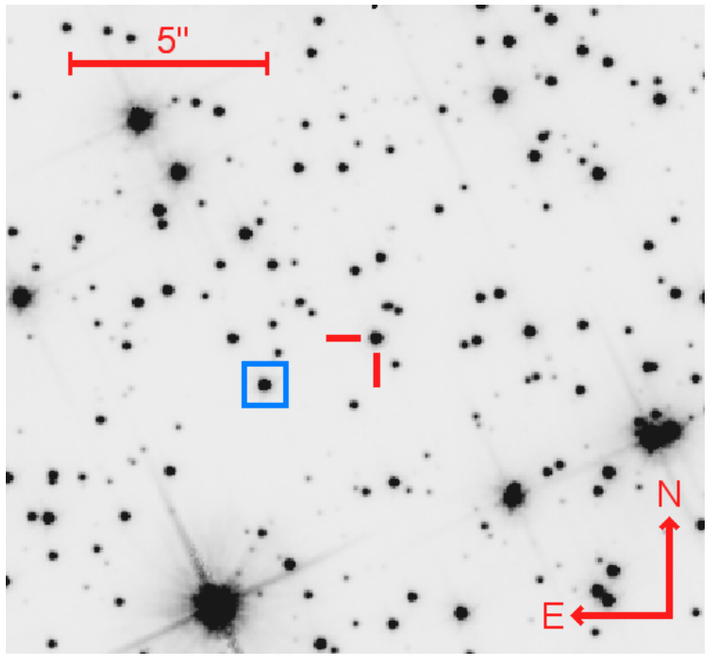

(a) HST

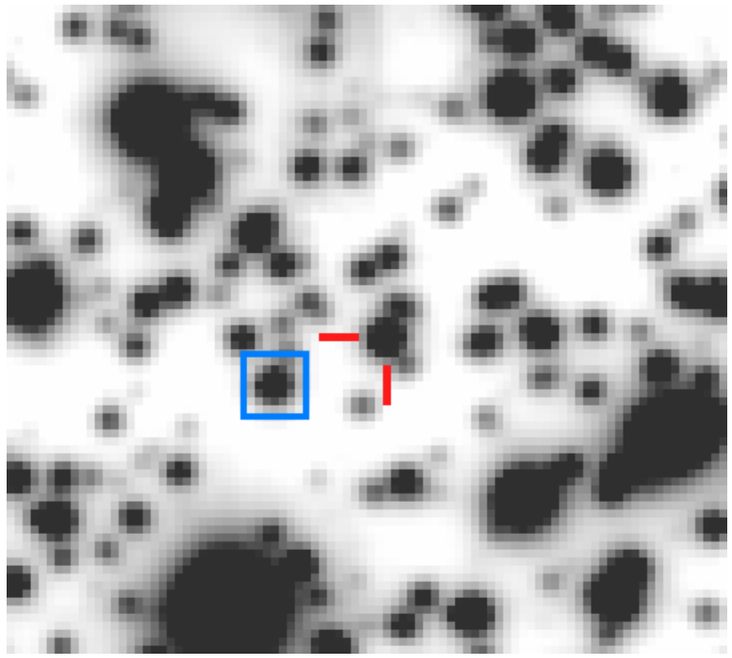

(b) MUSE

Galactic globular cluster NGC 3201 …

Stellar-mass BH identified through radial-velocity measurement

HST + VLT/MUSE observations infer a stellar-mass BH in the cluster from its (detached) binary companion

Giesers et al. 2018, MNRAS, 475, L15.

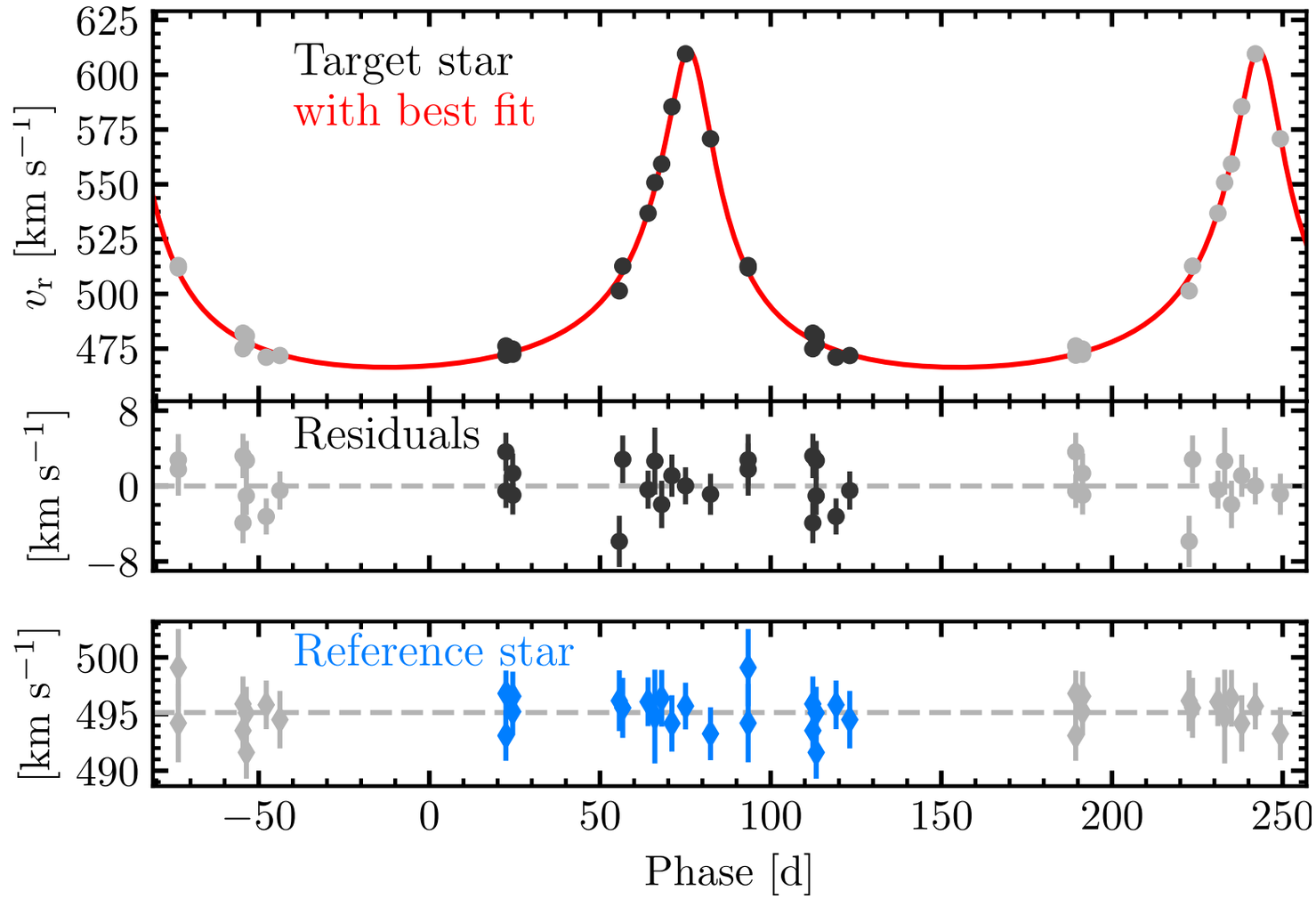

Model comparison with the observed structure and kinematics of globular clusters (GCs)

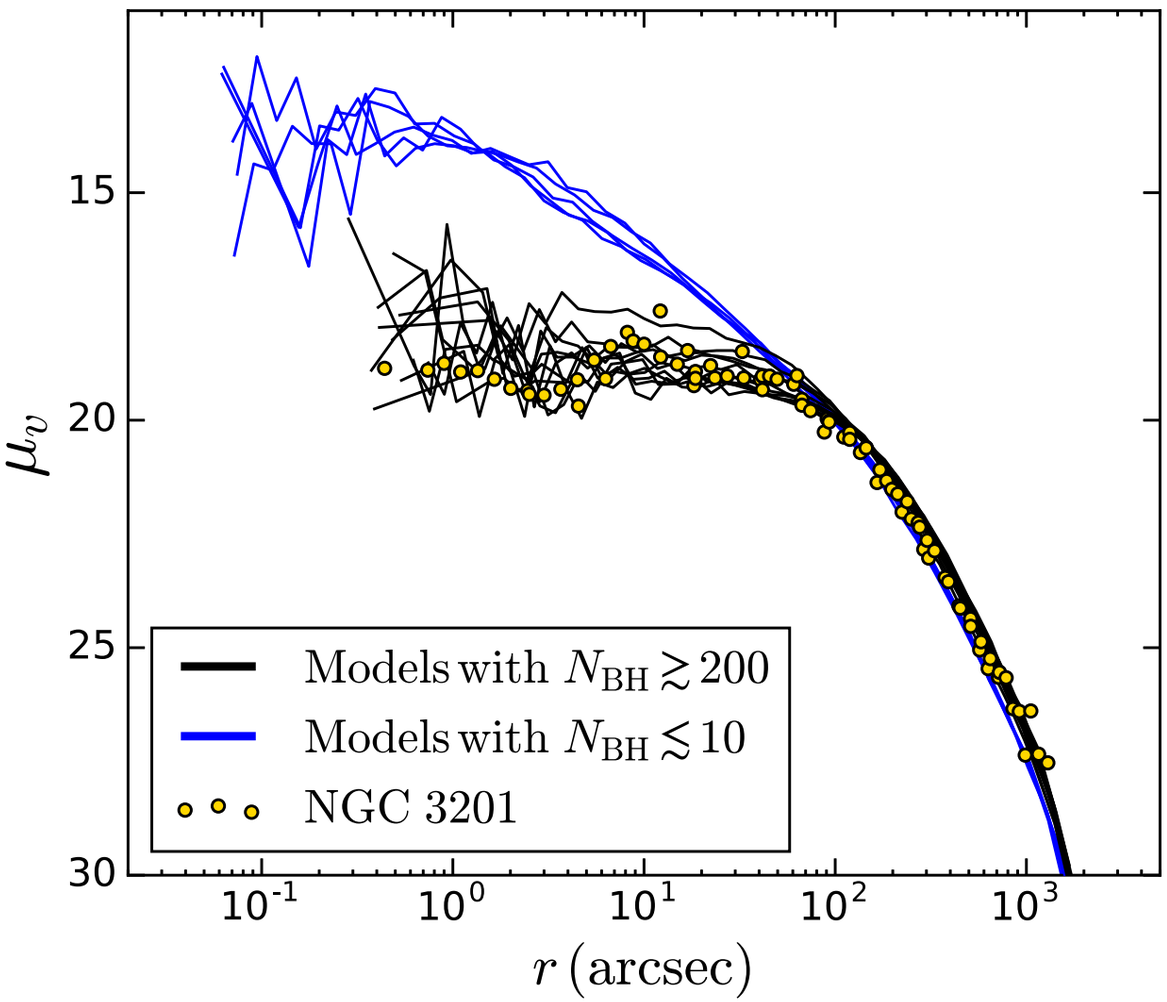

Modelling NGC 3201: Kremer at al. 2018, ApJ, 855, L15

Shortlisting BH population-containing Galactic GCs: Askar et al., 2018, MNRAS, 478, 1844

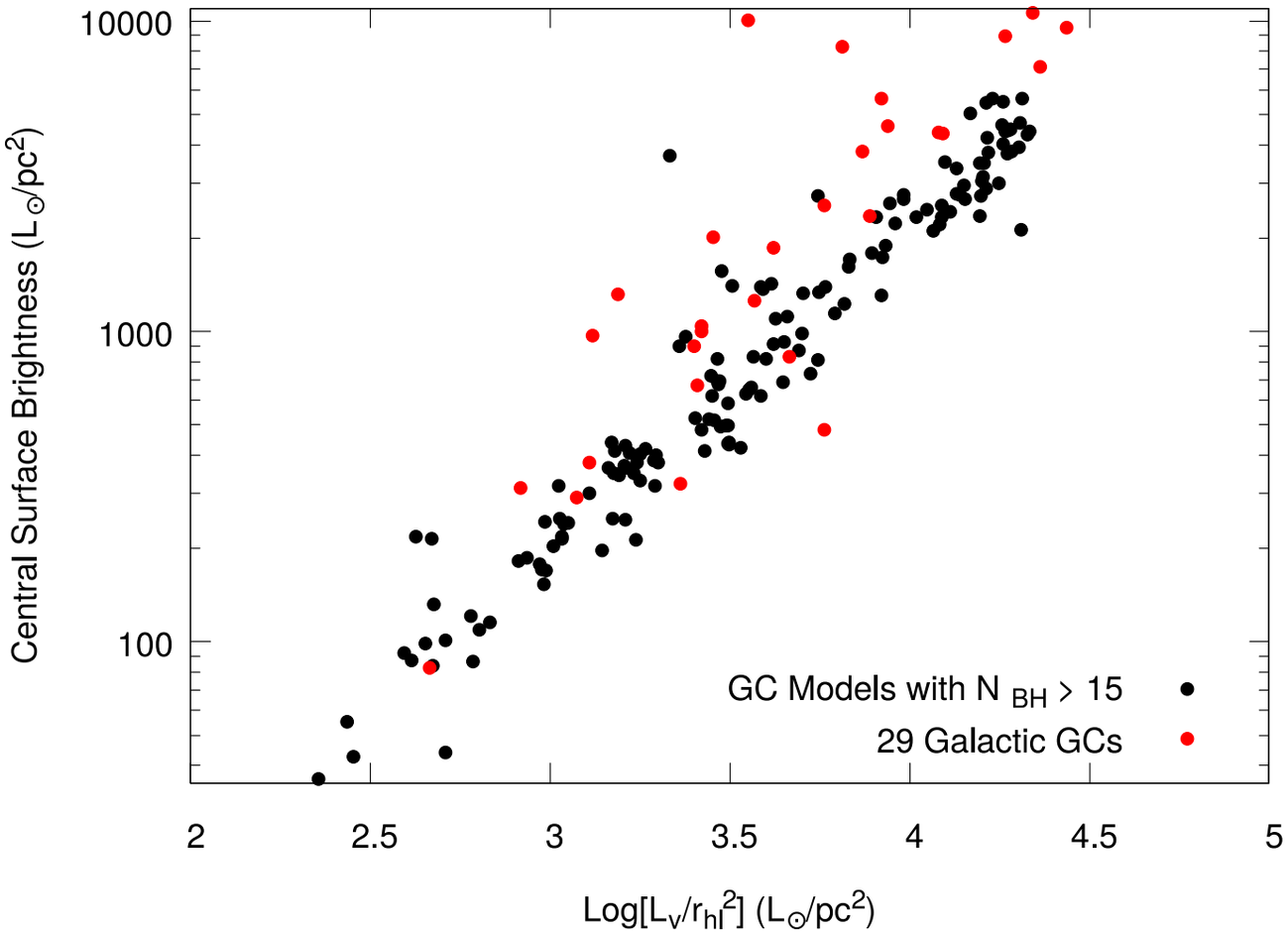

So, if a number of BHs retain in a cluster at birth what happens to them thereafter?

The virial theorem of self-gravitating systems

$$2T = -V$$

$T =$ total K.E. $\propto \frac{1}{2} M_{cl} \sigma^2$

$V =$ total P.E. $\propto -\frac{M_{cl}^2}{r_h}$

$M_{cl} =$ total cluster mass

$r_h =$ cluster half-mass radius

$$E = T + V = \frac{V}{2} \propto -\frac{M_{cl}^2}{r_h}$$

$$\sigma \propto \sqrt{\frac{M_{cl}}{r_h}}$$

=> negative specific heat

(if I extract energy, the system gets hotter!)

Evolving off the stable configuration: two-body relaxation

Two-body relaxation refers to the time evolution of a dynamical system due to the mutual energy exchange of the constituent members - the evolution due to the "granularity" of the internal gravitational force.

Local relaxation time at radius 'r':

$$t_r \approx \frac{0.065 v_m^3}{n m^2 G^2 \ln \Lambda} \quad [\ln \Lambda = \ln(p_{\max}/p_{90}) \sim 10]$$

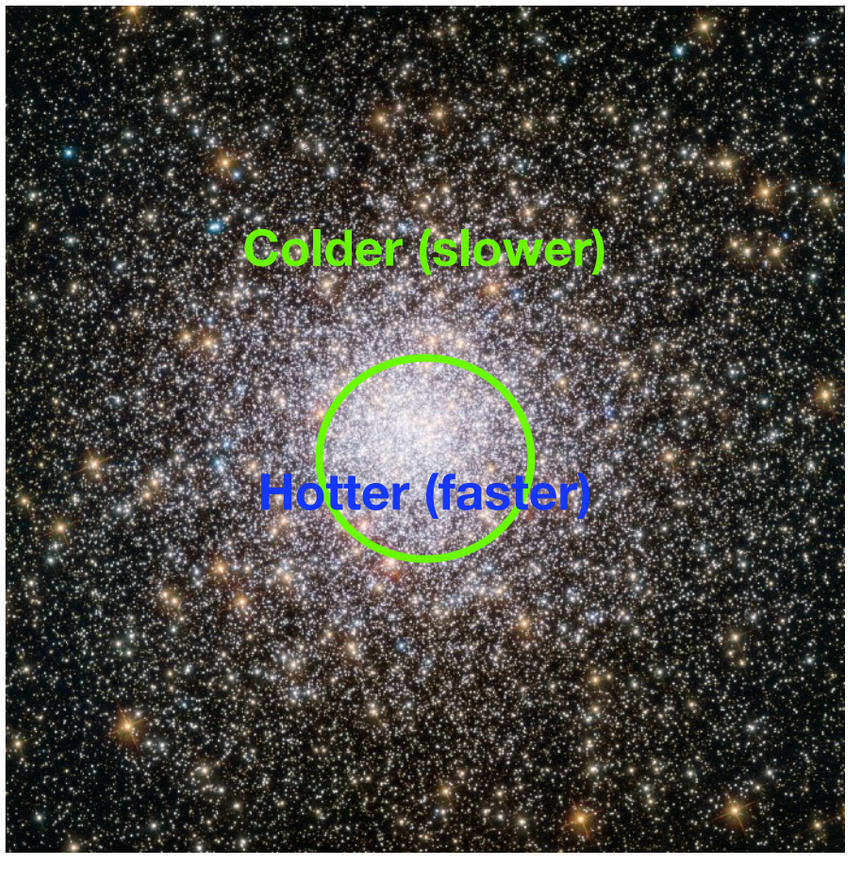

Relaxation time at half-mass radius assuming virial theorem:

$$t_{rh} \approx 0.138 \frac{N^{1/2} r_h^{3/2}}{m^{1/2} G^{1/2} \ln \Lambda}$$

In a (quasi) stable stellar configuration, relaxation leads to a net outward flow of energy/heat

See Spitzer (1987) book for the derivations

Two-body relaxation (cont)

$$t_{\rm rh} \propto N^{1/2}; \qquad r_h = \text{constant}$$

$$t_{\rm rh} \propto n^{-1/2}; \qquad N = \text{constant}$$

$$t_{rh} \sim \begin{cases} \text{Gyr} & \text{(young massive/open clusters)} \\ \text{Gyr} - t_{\rm Hubble} & \text{(globular clusters)} \\ \gtrsim t_{\rm Hubble} & \text{(nuclear clusters, dwarf galaxies, UCDs, ellipticals)} \end{cases}$$

Core collapse

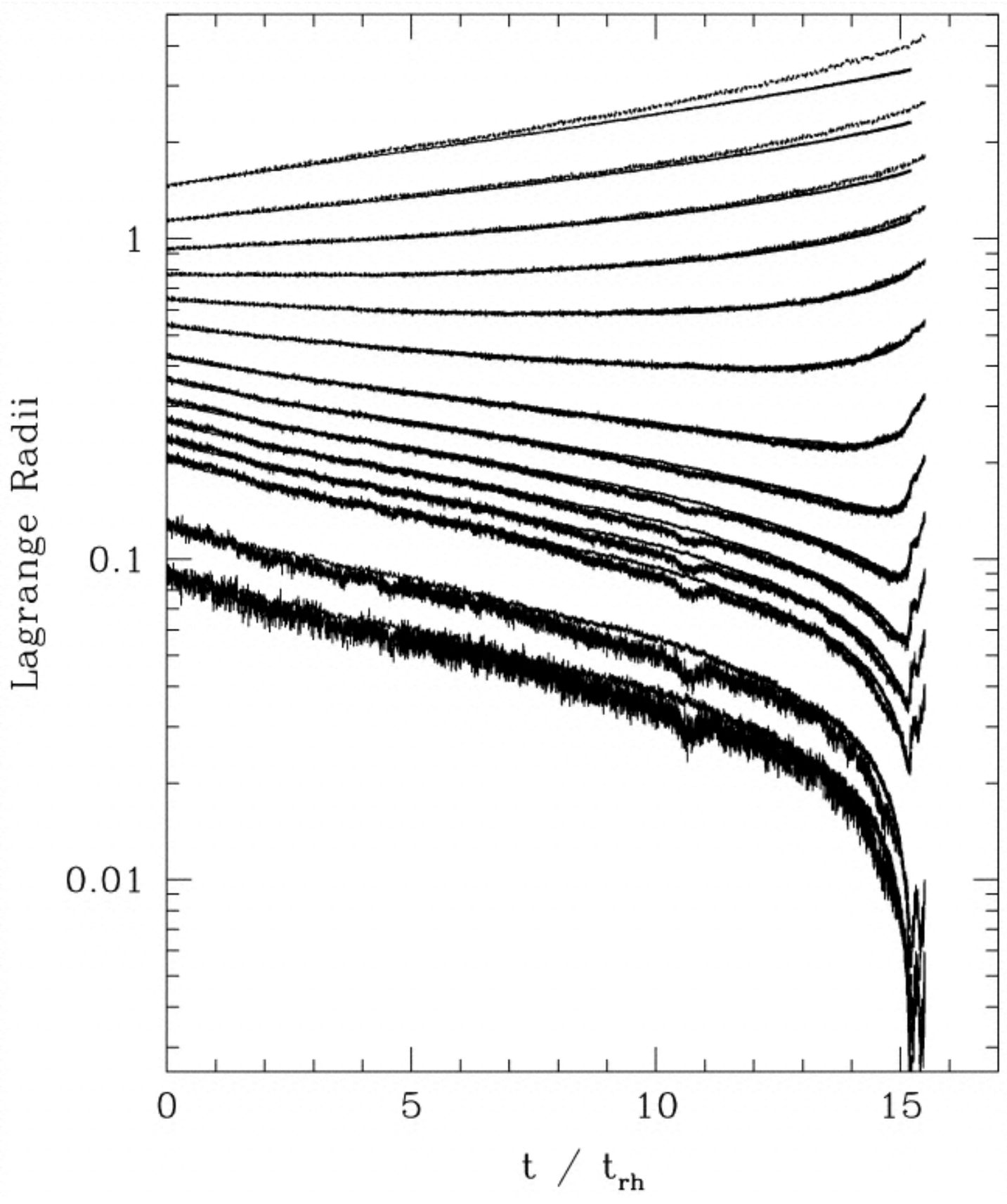

Runaway contraction of the core of a star cluster due to *gravothermal instability* in the final phase of dynamical relaxation.

Core-collapse of model cluster (tidally truncated $W_0 = 3$ King model) without primordial binaries & no stellar evolution.

Monte-Carlo computation superposed with corresponding N-body computation.

From Joshi et al. (2000).

$$t_{\rm cc} \approx 15 t_{\rm rh}(0)$$

Multi-mass systems: energy equipartition

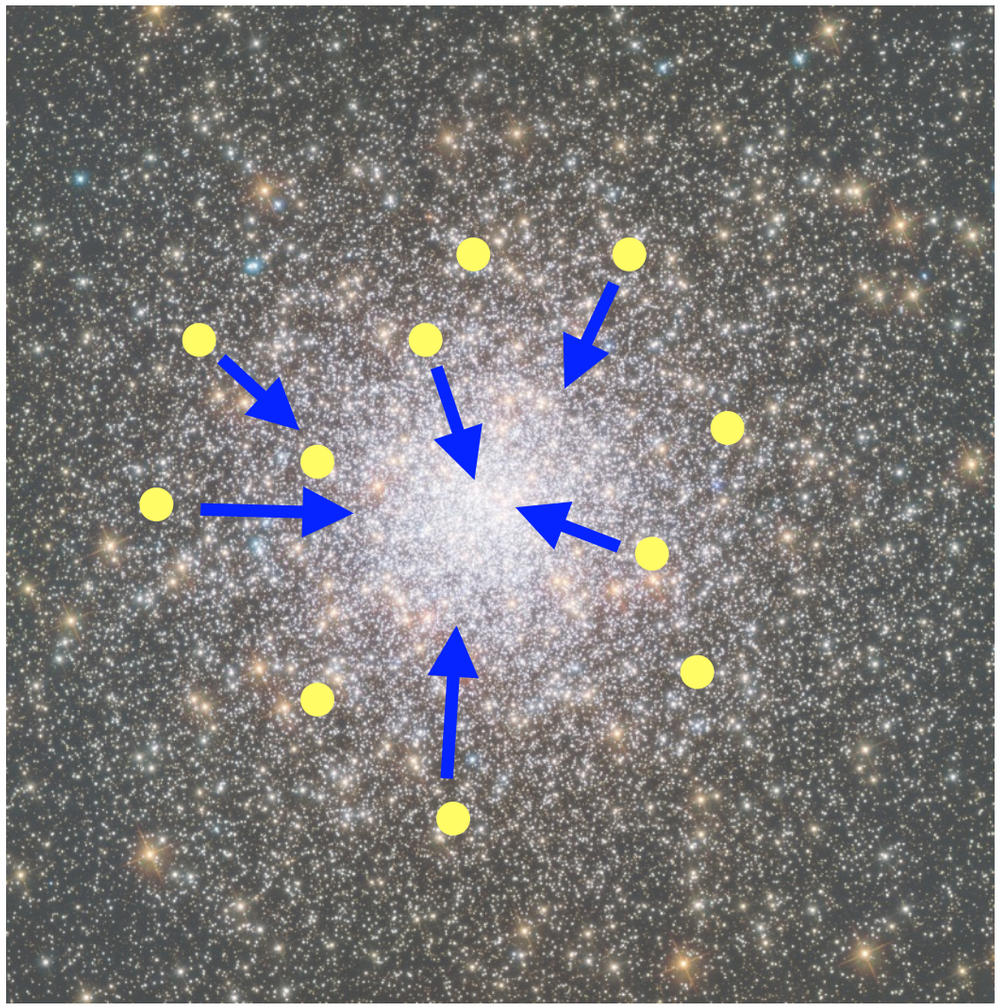

Two-body energy exchange leads to **energy equipartition** among various mass groups, simultaneously with relaxation.

(Tendency of)
Energy equipartition

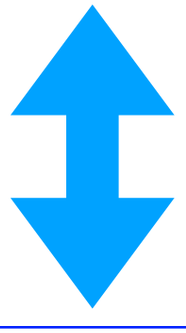

Mass segregation

Spatial separation among various mass groups: heavier entities occupy smaller radii

$$\frac{t_{\rm eq}}{t_{r1}} = \frac{3\pi^{1/2}}{16}\frac{m_1}{m_2}\left(1+\frac{\langle v_2^2\rangle}{\langle v_1^2\rangle}\right)^{3/2}, \qquad m_2 > m_1$$

$$\text{If } \langle v_1^2\rangle \approx \langle v_2^2\rangle, \quad \frac{t_{\rm eq}}{t_{r1}} \approx \frac{m_1}{m_2}$$

See,
Heggie & Hut (2003)
Spitzer (1987)

Multi-mass systems: mass stratification instability

If the more massive sub-group is sufficient in number and/or they are sufficiently heavy, they may never achieve energy equipartition.

This will cause continual / runaway sinking towards cluster center.

"Mass stratification" or "Spitzer" instability.

The Spitzer mass-stratification instability criterion:

$$\chi > \chi_{\max} = 0.16$$

$$\chi = \frac{M_2}{M_1}\left(\frac{m_2}{m_1}\right)^{\frac{3}{2}}$$

$m_1 =$ mass of background component
$m_2 =$ mass of heavier component
$M_X =$ total mass of component X

See Lyman Spitzer's book for a derivation.

Spitzer instability leads to a core-collapse of the heavier sub-group.

Taking $m_1 = m_* = 0.3, m_2 = m_{\rm BH} = 10.0$ as for the standard IMF

we have, for Spitzer Instability to occur,

$$\frac{M_{\rm BH}}{M_*} > 8.3 \times 10^{-4}$$

This can be easily achieved by retaining < 10 % of the stellar-mass BHs in the cluster after their birth.

The formation of a dense, central sub-cluster of BHs

$$t_{\rm seg,BH} \approx \frac{\langle m_* \rangle}{\langle m_{\rm BH} \rangle} t_{\rm cc} \qquad t_{\rm cc} \approx 15 t_{\rm rh}(0)$$

(If too few BHs retain, they would still remain centrally concentrated due to the dynamical friction of the background stars)

47 Tuc (credit NASA/ESA/HST)

Black hole engine!

47 Tuc (credit NASA/ESA/HST)

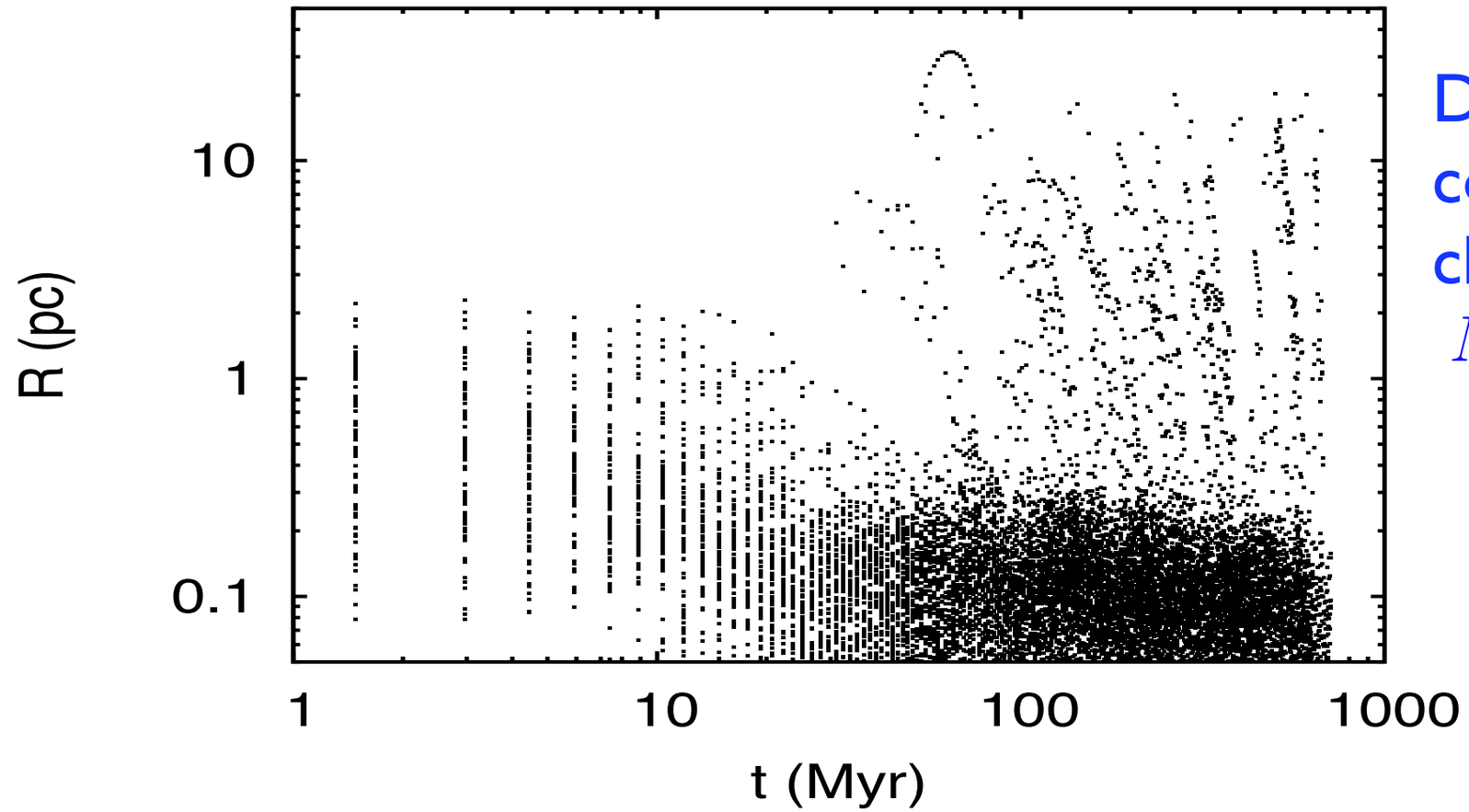

Direct N-body computation of $N = 4.5 \times 10^4$ cluster, $r_h(0) = 1$ pc, $N_{BH} \approx 100$ (full retention).

Banerjee, S., et al., 2010, MNRAS, 402, 371

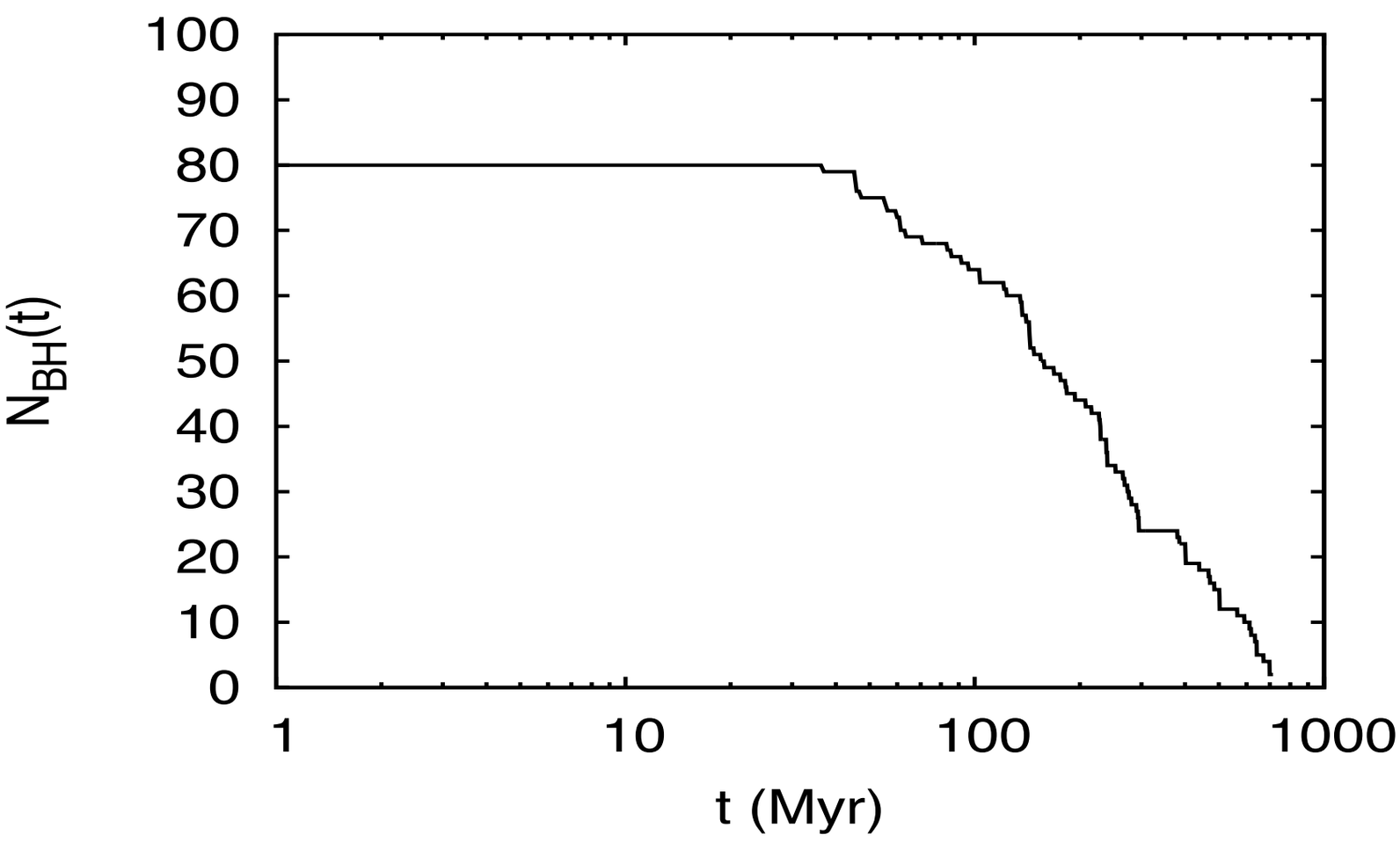

Two phases: (a) initial segregation: $N_{BH} \approx$ const (b) formation of BH-core: N_{BH} depletes due to super-elastic dynamical encounters.

BH-core (or "Dark core") phase have potential for a wide variety of physical phenomena

Multiple core collapse

~ Gyr - > Hubble time: Core-collapse of rest of the cluster

Not all episodes are necessarily directly observable!

see, e.g.,:

Morscher, M., et al., 2015, ApJ, 800, 9

Chatterjee, S., et al., 2017, ApJ, 834, 68

~ 100 Myr - Gyr : Core-collapse of BHs

~ Myr - 10 Myr: Core-collapse of massive stars

What happens after core collapse?

The core collapse (of a sub-component) can only be halted (or reversed) once dynamical energy-generation processes in the collapsed core begin

Energy generation occurs due to close binary-single interactions (more on Lecture 2!)

Leads to an overall expansion of the cluster

Post-core-collapse dynamical evolution is self-regulatory:
"central (dynamical) energy generation of a (post-core-collapse) cluster is controlled by the energy demands of the bulk of the cluster"
- He´non M., 1975, Proc. IAU Symp. Vol. 69, p.133 (the He´non's principle)

Self-similar model (see Spitzer or Heggie & Hut; use the relaxation time formula):

$$M_{\rm cl} \propto t^{-\nu}$$

$$r_h \propto t^{(2+\nu)/3}$$

$$v_m^2 \propto t^{-(2+4\nu)/3}$$